Table 1
Primer sequences and RT-PCR parameters

Genes	Primer sequence 5′–3′	PCR parameters[a]
HGF	F: AGGAGCCAGCCTGAATGATGA R: CCCTCTGATGTCCCAAGATTAGC	95, 56, 72 1 min, 45 s, 1 min
TGFα	F: ATGGTCCCCTCGGCTGGA R: GGCCTGCTTCTTCTGGCTGGCA	95, 59, 72 45 s, 30 s, 1 min
TGFβ1	F: GCCCTGGACACCAACTATTGCT R: AGGCTCCAAATGTAGGGGCAGG	95, 58, 72 45 s, 30 s, 1 min
TGFβ2	F: GATTTCCATCTACAAGACCACGAGGGACTTGC R: CAGCATCAGTTACATCGAAGGAGAGCCATTCG	95, 58, 72 45 s, 30 s, 1 min
HGFR	F: TGGTCCTTGGCGTCGTCCTC R: CTCATCATCAGCGTTATCTTC	95, 54, 72 30 s, 45 s, 1 min
EGFR	F: CTACCACCACTCTTTGAACTGGACCAAGG R: TCTATGCTCTCACCCCGTTCCAAGTATCG	95, 58, 72 45 s, 30 s, 1 min
TGFβ1R	F: CGTGCTGACATCTATGCAAT R: AGCTGCTCCATTGGCATAC	95 s, 54, 72 30 s, 45 s, 1 min
TGFβ2R	F: TGCACATCGTCCTGTGGAC R: GTCTCAAACTGCTCTGAAGTGTTC	95, 58, 72 45 s, 30 s, 1 min
FGFR	F: ATGTGGAGCTGGAAGTGCCTC R: GGTGTTATCTGTTTCTTTCTCC	95, 54, 72 30 s, 45 s, 1 min
IGF-1R	F: ACCCGGAGTACTTCAGCGCT R: CACAGAAGCTTCGTTGAGAA	95, 54, 72 30 s, 45 s, 1 min
HNF1α	F: GTGTCTACAACTGGTTTGCC R: TGTAGACACTGTCACTAAGG	95, 52, 72 45 s, 30 s, 1 min
HNF1β	F: GAAACAATGAGATCACTTCCTCC R: CTTTGTGCAATTGCCATGACTCC	95, 52, 72 1 m, 45 s, 1 min
HNF3β	F: CACCCTACGCCTTAACCAC R: GGTAGTAGGAGGTATCTGCGG	95, 56, 72 1 m, 45 s, 1 min
HNF4	F: CTGCTCGGAGCCACAAAGAGATCCATG R: ATCATCTGCCACGTGATGCTCTGCA	95, 58, 72 45 s, 30 s, 1 min
Albumin	F: AGTTTGCAGAAGTTTCCAAGTTAGTG R: AGGTCCGCCCTGTCATCAG	95, 55, 72 45 s, 30 s, 1 min
Apolipoprotein-a	F:AGGCTCGGCATTTCTGGCAG R: TATCCCAGAACTCCTGGGTC	95, 55, 72 45 s, 30 s, 1 min
HTF	F: TCGCTACAGCCTTTGCAATG R: TTGAGGGTACGGAGGAGTTCC	95, 55, 72 45 s, 30 s, 1 min
E-cadherin	F: TCCATTTCTTGGTCTACGCC R: TTTGTCCTACCGACTTCCAC	95, 55, 72 45 s, 30 s, 1 min
CYP 1B1	F: CACCAAGGCTGAGACAGTGA R: GCCAGGTAAACTCCAAGCAC	94, 57, 72 30 s, 30 s, 1 min
CYP 2C9	F: GGACAGAGACGACAAGCACA R: TGGTGGGGAGAAGGTCAAT	94, 57, 72 30 s, 30 s, 1 min
CYP 2B	F: GGCACACAGCCAAGTTTACA R: CCAGCAAAGAAGAGCGAGAG	94, 57, 72 30 s, 30 s, 1 min
CYP 3A4	F: TGTGCCTGAGAACACCAGAG R: GCAGAGGAGCCAAATCTACC	94, 57, 72 30 s, 30 s, 1 min
CYP 2E1	F: CCGCAAGCATTTTGACTACA R: GCTCCTTCACCCTTTCAGAC	94, 57, 72 30 s, 30 s, 1 min
CYP 1A1	F: AGGCTTTTACATCCCCAAGG R: GCAATGGTCTCACCGATACA	94, 57, 72 30 s, 30 s, 1 min
GAPDH	F: CCATGGAGAAGGCTGGGG R: CAAAGTTGTCATGGATGACC	95, 8, 72 45 s, 30 s, 1 min

Table 1 (*continued*)

Genes	Primer sequence 5′–3′	PCR parameters[a]
CD81	F: CTCAACTGTTGTGGCTCCAAC R: CCAATGAGGTACAGCTTCCC	95, 55, 72 45 s, 30 s, 1 min
TLR3	F: GATCTGTCTCATAATGGCTTG R: GACAGATTCCGAATGCTTGTG	95, 55, 72 45 s, 30 s, 1 min
TLR7	F: CCAGACATCTCCCCAGCGTC R: GGCAAAACAGTAGGGACGGC	95, 55, 72 45 s, 30 s, 1 min
TLR8	F: CTGTGAGTTATGCGCCGAAG R: CGGGATTTCCGTTCTGGTGC	95, 55, 72 45 s, 30 s, 1 min
Myd88	F: GGTCTCCTCCACATCCTCCC R: CCAGCTTGGTAAGCAGCTCG	95, 55, 72 45 s, 30 s, 1 min
IRF3	F: GAACCCCAAAGCCACGGATC R: CCTCCCGGGAACATATGCAC	95, 55, 72 45 s, 30 s, 1 min
IRF7	F: GTGCTGTTCGGAGAGTGGCTC R: CAGCCCAGGCCTTGAAGATG	95, 55, 72 45 s, 30 s, 1 min

CYP, cytochrome P450; EGFR, epidermal growth factor receptor; F, forward primer; FGFR, fibroblast growth factor receptor; GAPDH, glyceraldehyde phosphate dehydrogenase; HGF, hepatocyte growth factor; HGFR, hepatocyte growth factor receptor; HNF, hepatocyte nuclear factor; HTF, human transferrin; IGF-1R, insulin-like growth factor-type I receptor; IRF, interferon regulatory factor; R, reverse primer; TGF, transforming growth factor; TGFR, transforming growth factor receptor; TLR, toll like receptor.

[a] Temperatures are tabulated in the first lane in degrees celsius and the corresponding times in the second lane. Performing one-step RT-PCR, reverse transcription was carried out at 42 °C for 20 min with a pre-PCR denaturation at 95 °C for 10 min.

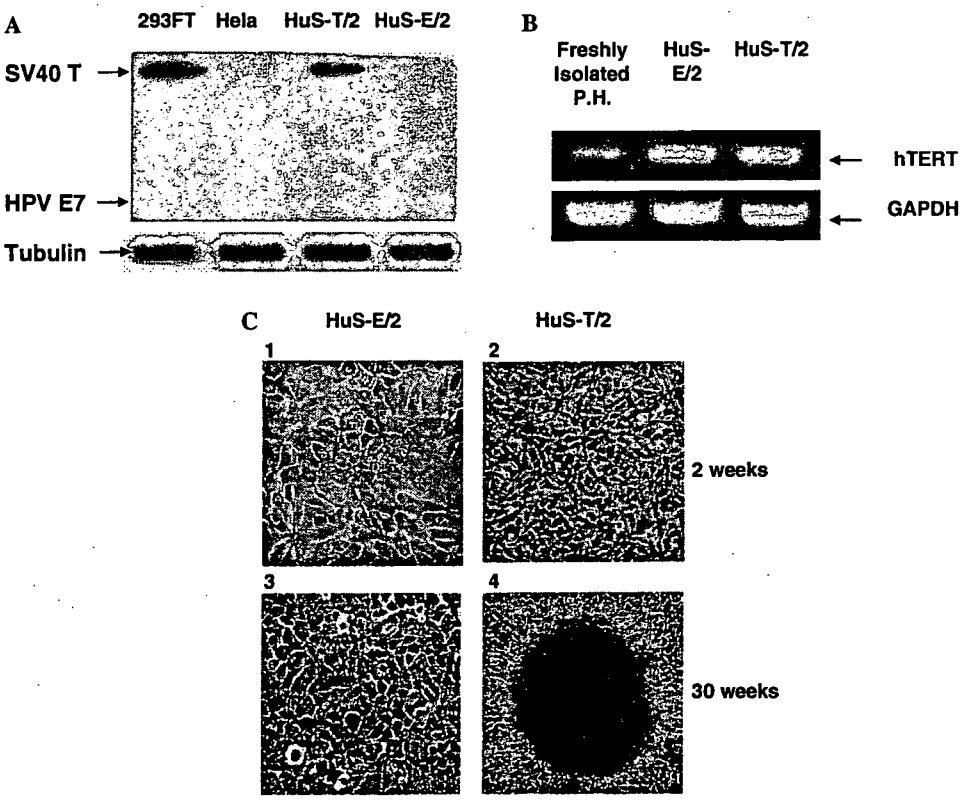

Fig. 1. (A) Immunoblot detection of SV40 T and HPV E7 expression in HuS-T/2 and HuS-E/2 cells, respectively. 293-FT and HeLa cells were used as positive controls for SV40 T and HPV E7 expression, respectively. The specific bands representing the targets are indicated. Detection of tubulin expression in all cells served as an internal control. (B) Human Telomerase Reverse Transcriptase (hTERT) expression was examined by RT-PCR in freshly isolated hepatocytes and the HuS-E/2 and HuS-T/2 cell lines. GAPDH expression was used as an internal control. The hTERT-specific bands are shown. (C) Morphological characteristics of HuS-E/2 and HuS-T/2 cells after two (panels 1 and 2) and 30 (panels 3 and 4) weeks in culture. [This figure appears in colour on the web.]

while the HPV18/E6E7-immortalized clones were named HuS-E cells and given numbers from 1 to 4. Expression of SV40 T and HPV E7 proteins was detected in the appropriate cells by immunoblot analysis (Fig. 1A). In both immortalized cell lines, expression of hTERT-mRNA was enhanced in comparison to non-transduced, freshly isolated hepatocytes as determined by RT-PCR (Fig. 1B). HuS-E cells were larger in size and exhibited slower growth than HuS-T cells (Fig. 1C).

3.2. Characterization of HuS-E and HuS-T immortalized hepatocytes

The HuS-E/2 and HuS-T/2 clones demonstrated the highest expression of hepatocyte-specific markers and transcription factors by RT-PCR (data not shown); these cells were used as representative for each group in this study. To address if HuS-E/2 and HuS-T/2 maintained similar characteristics as primary hepatocytes, they were both cultured continuously for 30 weeks and the expression profiles of a variety of growth factors (Fig. 2A), growth factor receptors (Fig. 2B), hepatocyte-specific nuclear factors (Fig. 2C), albumin, apolipoprotein-A1, transferrin (Fig. 2D), cytochrome p450 (CYP) genes (Fig. 2E), and GAPDH were compared with freshly isolated primary hepatocytes after isolation or two weeks of culture, Huh-7.5 cells, and 293 cells. After two weeks in culture, the expression of nearly all examined genes was similar between freshly isolated hepatocytes and the HuS-E/2 cell line. HuS-E/2 cells, however, exhibited higher expression of TGFβ2 (Fig. 2A), TGFβ2R, and HGFR (Fig. 2B) and lower expression of CYP 3A4 and 2C9 (Fig. 2E) in comparison to freshly isolated hepatocytes. Primary hepatocytes displayed reduced expression of TGFβ1 and TGFβ2 (Fig. 2A) and a loss of CYP1A1 expression (Fig. 2E) after two weeks of culture. HuS-E/2 cells exhibited higher expression of HGF (Fig. 2A), HGF receptor (Fig. 2B), HNF-4, (Fig. 2C), albumin, apolipoprotein-A1, HTF, and E-cadherin (Fig. 2D) in comparison to HuS-T/2 cells. Expression of CYP 3A4 (Fig. 2E) was lost from both HuS-T/2 and HuS-E/2 cells, while HuS-T/2 cells also lost the expression of HNF-1α (Fig. 2D), and CYPs 2B, 2E1 (Fig. 2E).

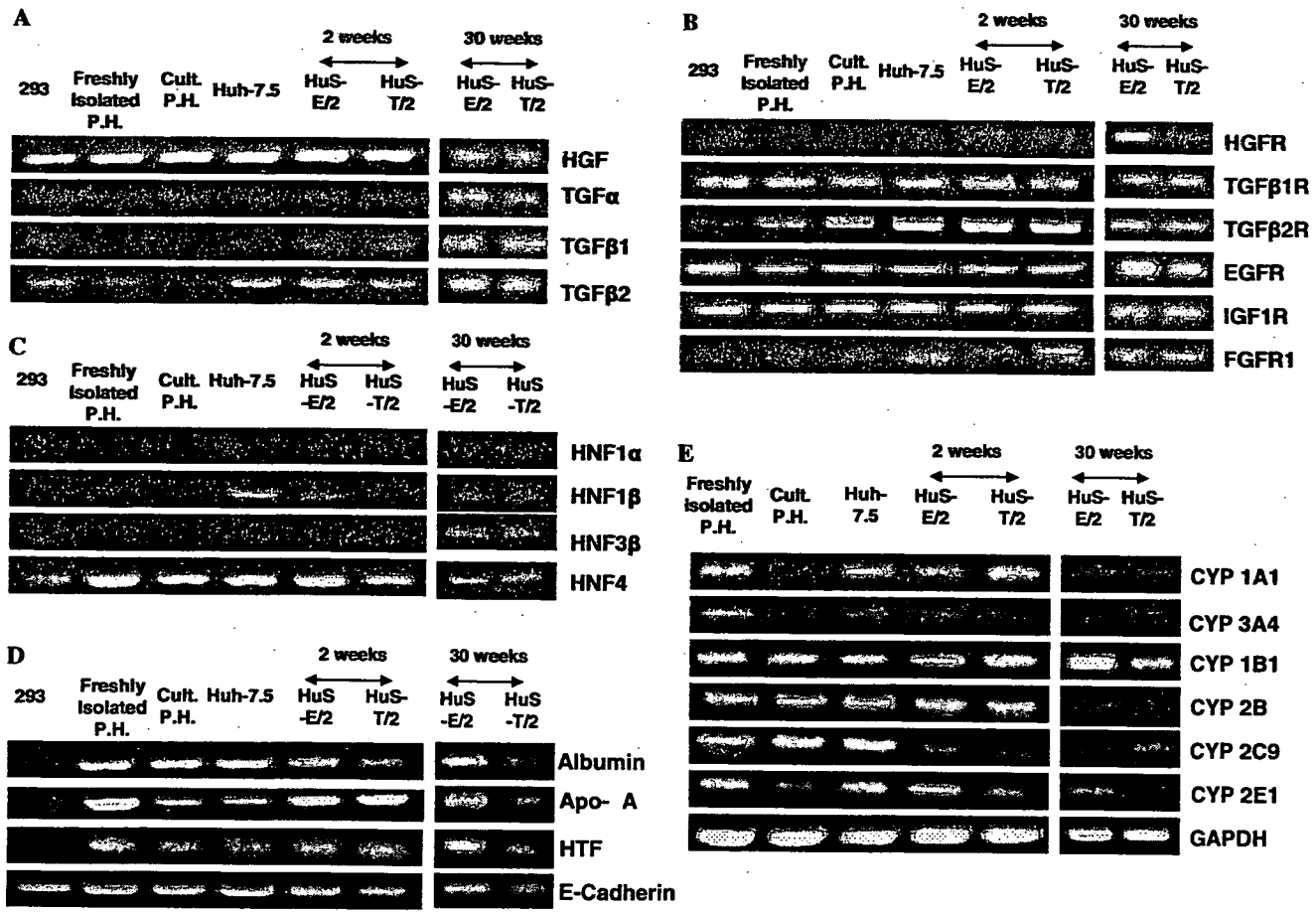

Fig. 2. Expression of the genes encoding growth factors (A), growth factor receptors (B), hepatocyte-specific nuclear factors (C), hepatocyte differentiation and functional markers (D), and CYP enzymes (E) in 293 cells, freshly isolated primary hepatocytes (P.H.), primary hepatocytes cultured for two weeks (Cult. P.H.), Huh-7.5 cells, and HuS-E/2 and HuS-T/2 cells cultured for two and 30 weeks were investigated by RT-PCR. The bands representing specific targets are indicated in the representative reactions.

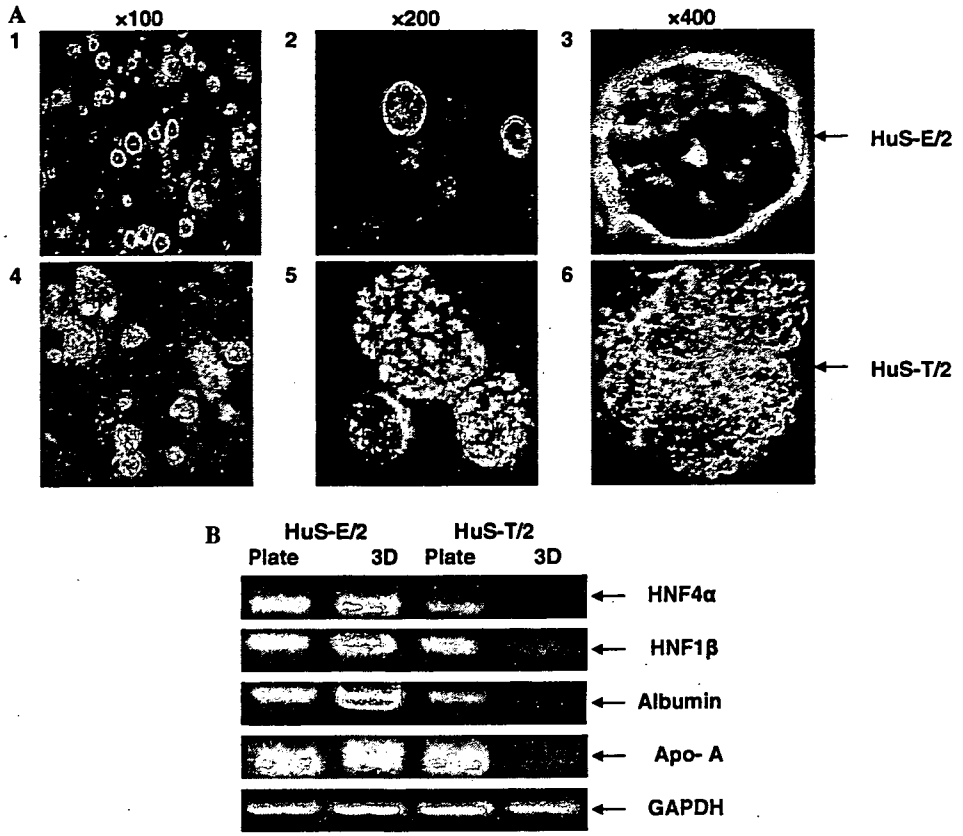

Fig. 3. (A) The morphology of HuS-E/2 and HuS-T/2 cells in 3D culture. HuSE/2 and HuS-T/2 cells were cultured in Mebiol Gel in 12-well plates at a concentration of 5×10^5 cells/well. The microscopic characteristics of these cells after one week of 3D culture are shown. (B) The expressions of HNF4α, HNF1β, albumin, and apo-A by HuS-E/2 and HuS-T/2 cells in both flat and 3D cultures are detailed. After one week of culture of HuS-E/2 and HuS-T/2 cells in flat and 3D cultures, the expressions of HNF4α, HNF1β, albumin, and apo-A were measured by RT-PCR in 250 ng total RNA.

HuS-T/2 but not in HuS-E/2 cells showed a transformed-like character starting from the 13th week of culture. This was demonstrated by continuing proliferation after confluence, pile-up formations (Fig. 1C), and proliferating in serum-deprevied condition. However, HuS-E/2 cells did not show any transformed-like characters even after 30 weeks of culture.

3.3. The characteristics of HuS-E and HuS-T immortalized hepatocytes in 3D culture

After one week in 3D culture, HuS-E/2 (Fig. 3A, panels 1, 2, and 3) cells adopted a donut-shaped structure with a central pore, while HuS-T/2 cells (Fig. 3A, panels 4, 5, and 6) displayed irregular mass formations (similar to the growth pattern of Huh-7.5 cells in 3D culture (data not shown)). In 3D culture, while the expression of HNF4, HNF1β, and albumin was enhanced in HuS-E/2, it was decreased in HuS-T/2 cells (Fig. 3B).

3.4. HCV infection to HuS-E/2

We further assessed the HCV infectivity of HuS-E- and HuS-T-derived clones by infection with HCV-1b-infected serum. Of the three HuS-E clones examined, HuS-E/2 clone demonstrated the highest infectability with HCV genotype 1b in comparison to Huh-7.5, PH5CH8 (Fig. 4A), and HuS-T cells (data not shown), which were excluded from further experiments.

3.5. Anti-CD81 blocked HCV infectivity

CD81 is involved in the entry of HCV pseudoparticles [24] and in vitro-synthesized JFH-1 [7]. To determine if authentic viral particles follow the same route of entry when infecting HuS-E/2 cells, we first examined the CD81 expression by RT-PCR. Both HuS-E/2 and HuS-T/2 cells expressed similar amounts of CD81 as freshly isolated hepatocytes and Huh-7.5 cells (Fig. 4B). Antibodies against CD81 reduced HCV infectivity of HuS-E/2 cells from the levels seen using a non-specific control antibody, confirming the importance of CD81 in HCV infectivity (Fig. 4C).

3.6. IFNα blocked HCV infectivity

We treated HuS-E/2 cells with HCV-containing serum. Cells were then cultured in fresh medium supplemented

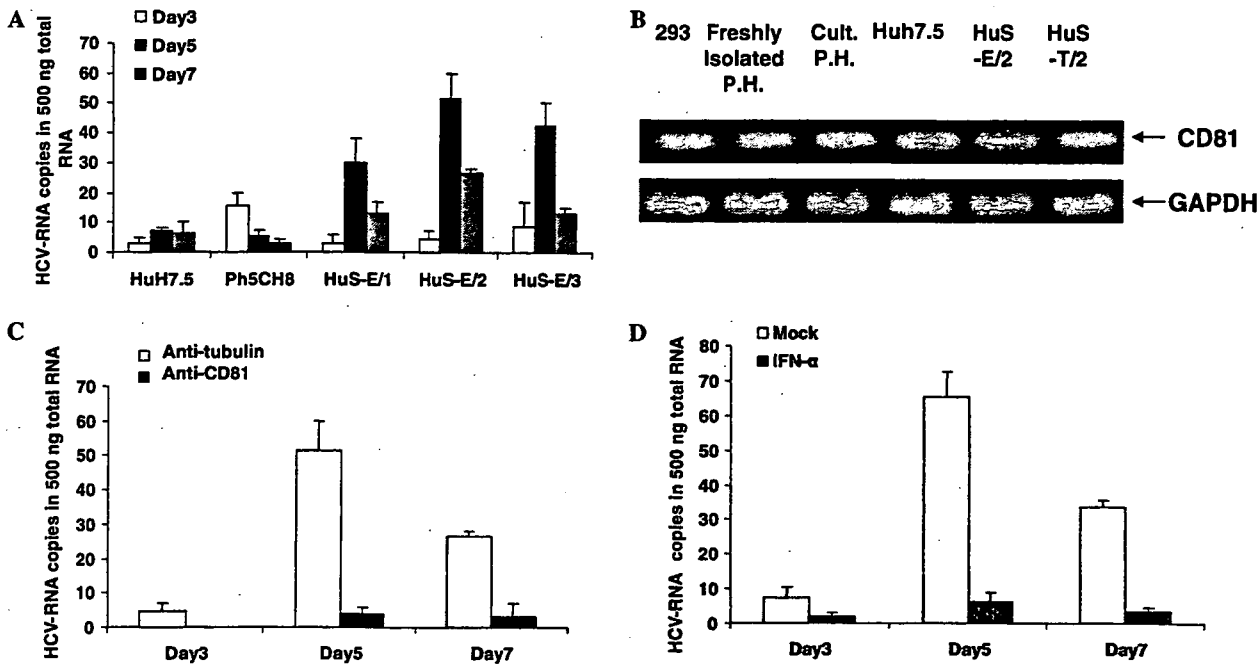

Fig. 4. (A) Serum from an HCV patient was used to infect Huh-7.5 cells, PH5CH8 cells, and three HPV E6E7-immortalized clones (HuS-E/1-3) for 24 h. After washing three times in phosphate-buffered saline (PBS), cells were cultured in fresh medium. Cells were then harvested and lysed at the indicated time points. The quantity of HCV genome RNA per 500 ng total RNA was determined by real-time RT-PCR analysis. (B) HuS-E/2 and HuS-T/2 cells both expressed CD81. Expression of CD81 (upper panel) and GAPDH as an internal control (lower panel) in 293 cells, freshly isolated P.H., cultured P.H., and Huh-7.5, HuS-E/2, and HuS-T/2 cells was investigated by RT-PCR. (C) Anti-CD81 antibodies blocked HCV infectivity. HCV infection was performed as described in (A) with the addition of CD81-specific (black bar) or anti-tubulin antibodies (control, white bar). (D) IFNα inhibits HCV multiplication in HuS-E/2 cells infected with HCV-containing serum. HuS-E/2 cells were infected with HCV as described in (A). After washing three times with PBS, cells were cultured in fresh medium supplemented with (black bar) or without (white bar) 100 U/ml IFNα.

without or with 100 U/ml IFNα. The enhancement of the HCV-RNA genome titers on the fifth day (about 10-fold) was not observed in cells treated continuously with IFNα (Fig. 4D). This result suggests that IFNα inhibited HCV replication in infected HuS-E/2 cells.

3.7. The effect of blocking IRF-3 and IRF-7 signaling on HCV infectivity

Production of interferon-alpha (IFNα) and interferon-beta (IFNβ) limits viral replication and spread, providing one of the most effective innate antiviral responses [25]. Signaling through IRF-3 and IRF-7 plays important roles in the stimulation of IFN-α/β production [25]. To determined which molecules (IRF-3 or IRF-7) play an important role in modulation of the innate immune response against HCV infection in these cells, we first detected intrinsic expression of double-stranded RNA-stimulated Toll-like receptor (TLR) 3, the downstream effector IRF-3, single-stranded RNA-stimulated TLR7, and 8, and the downstream effectors MyD88 and IRF-7 by RT-PCR. TLR3 exhibited very low expression in freshly isolated hepatocytes, Huh-7.5, HuS-E/2, and HuS-T/2 cells, while TLR7, TLR8, MyD88, and IRF-7 were easily detectable in both freshly isolated and immortalized cell lines (Fig. 5A).

The abilities of DNIRF-3 and DNIRF-7 to inhibit IFNβ and IFNα production by HuS-E/2 cells infected with Sendai virus were confirmed using assays of IFNβ or IFNα promoter-driven luciferase reporters. DNIRF-3 exhibited strong inhibition of IFNβ production (Fig. 5B) and weaker inhibition of IFNα transcription (Fig. 5C), while DNIRF-7 strongly inhibited IFNα production (Fig. 5C) and only weakly inhibited IFNβ production (Fig. 5B).

We then assessed the inhibition of HCV infectivity by DNIRF-3 and DNIRF-7. Transient transfection with DNIRF-3, DNIRF-7, or an empty vector was performed prior to HCV infection. Using Effectene reagent, the efficiency of plasmid transfection into HuS-E/2 cells was approximately 70% (data not shown). While there was no significant effect of DNIRF-3 on HCV infectivity, DNIRF-7 demonstrated a marked increase in HCV titers on days 3 and 5 after infection in comparison to control cells (Fig. 5D). To confirm that the enhancement of HCV replication by DNIRF-7 is not mediated by the impairment of IRF-3 signaling by heterodimeric interactions between IRF-3 and DNIRF-7, we performed siRNA inhibition of IRF-3 and IRF-7. The reduction of IRF-3 and IRF-7 expression by siRNA was obvious by RT-PCR (Fig. 5E). siRNA-mediated suppression of either IRF-3 or IRF-7 inhibited IFNβ and IFNα production

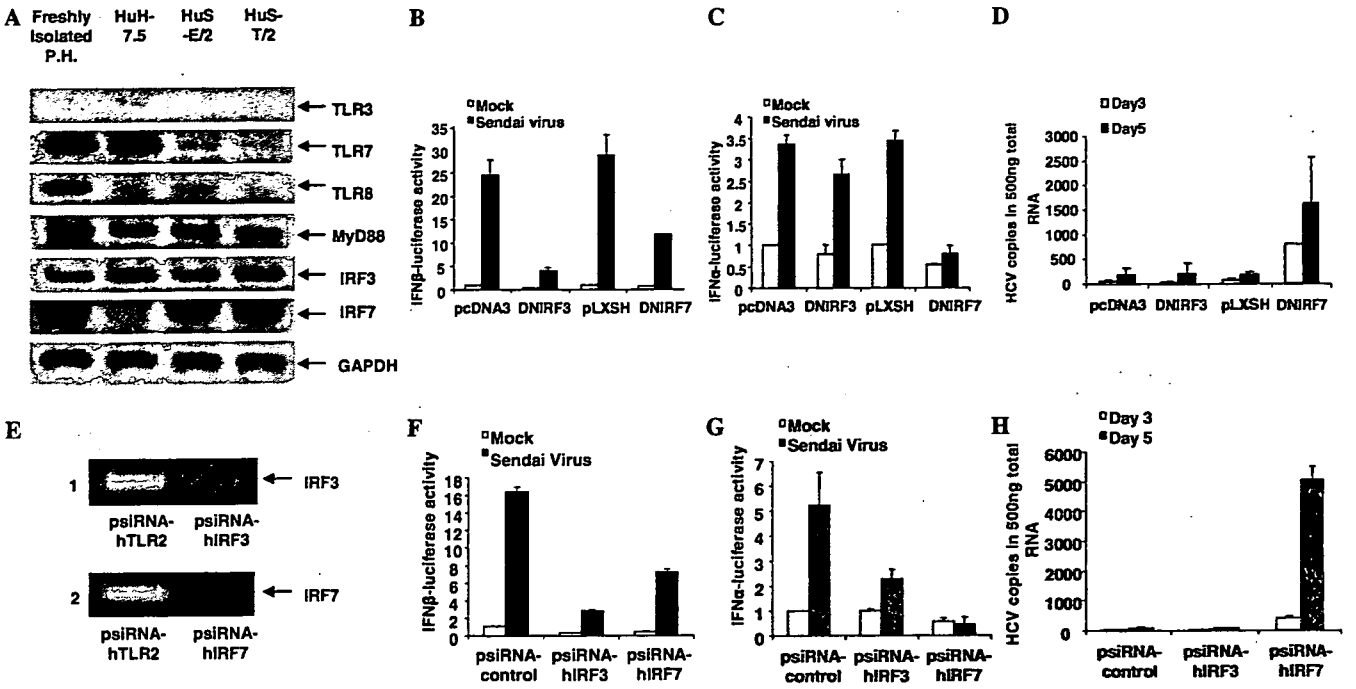

Fig. 5. (A) We examined the expression of TLR3, TLR7, TLR8, MyD88, IRF-3, and IRF-7, as well as GAPDH as an internal control in freshly isolated primary hepatocytes and Huh-7.5, HuS-E/2, and HuS-T/2 cells was investigated by RT-PCR. (B and C) HuS-E/2 cells were cotransfected with pIFNβ-luc (B) or pIFNα-luc (C) with an expression plasmid encoding DNIRF-3, DNIRF-7, or the appropriate empty vector (pcDNA3 and PLXSH, respectively). Twenty-four hours later, cells were infected (black bar) with Sendai virus or mock-infected (white bar), then analyzed for luciferase activity after 12 h. (D) IRF-7, but not IRF-3, suppression enhanced HCV infectivity of HuS-E/2 cells. HuS-E/2 cells were transiently transfected with empty pcDNA3, DNIRF-3, empty pLXSH, or DNIRF-7 plasmids. Twenty-four hours later, serum from a patient with HCV was used to infect transfected cells for 24 h. After washing, cells were cultured in fresh medium. The cells were then harvested and lysed at the indicated time points. The quantity of HCV genome RNA per 500 ng total RNA was determined by real-time RT-PCR analysis. (E) IRF-3 and IRF-7 levels were suppressed by specific siRNAs. HuS-E/2 cells were transfected with control psiRNA-hTLR2, psiRNA-hIRF-3, or psiRNA-hIRF-7, then selected with Zeocin at 250 μg/ml. Two weeks later, cells were harvested and assessed for the expression of IRF-3 and IRF-7 by RT-PCR. (F and G) HuS-E/2 cells were transfected with control psiRNA-hTLR2, psiRNA-hIRF-3, or psiRNA-hIRF-7, followed by selection in Zeocin at 250 μg/ml. Two weeks later, cells were cotransfected with pIFNβ-luc (F) or pIFNα-luc (G). Twenty-four hours later, cells were infected (black bar) with Sendai virus or mock-infected (white bar), then analyzed for luciferase activity after 12 h. (H) Transfected cells were infected with serum from HCV patient; HCV infectivity was assessed as described above.

in HuS-E/2 cells infected with Sendai virus in patterns similar to the effects seen following DNIRF-3 and DNIRF-7 expression, respectively (Figs. 5F and G). Blockade of IRF-7 expression resulted in a significantly higher titer of HCV after infection, while IRF-3 down-regulation did not have any significant effect on HCV titers (Fig. 5H). The enhancement of IRF-7 silencing by siRNA improved the infectivity of HCV (data not shown). These results suggest that IRF-7 plays the major role in the innate immune response to HCV in HuS-E/2 cells.

3.8. Establishment of stable DNIRF-7 expressing clones derived from HuS-E/2 cells

Since DNIRF-7 enhanced HCV infectivity, we transduced the plasmid encoding DNIRF-7 and a hygromycin-B resistance gene, into HuS-E/2 cells. Following selection with hygromycin-B, we obtained the HuS-E7/DN22 and HuS-E7/DN24 clones. As detected by RT-PCR, both clones demonstrated similar expression levels of albumin, apolipoprotein-A1, and HNF4 as the parental HuS-E/2 cells (Fig. 6A). The HuS-E7/DN24 clone exhibited stronger expression of DNIRF-7 than the HuS-E7/DN22 clone by immunoblotting (Fig. 6B). The induction of IFNα in HuS-E7/DN24 in response to infection with an RNA virus (Sendai virus) was low in comparison to the parental HuS-E/2 and HuS-E7/DN22 clones, as detected by IFNα-luciferase reporter assay (Fig. 6C). HuS-E7/DN24 also exhibited a higher HCV infectability in comparison to parental HuS-E/2 cells and the HuS-E7/DN22 clone (Fig. 6D).

3.9. Infection of HuS-E7/DN24 cells with different HCV genotypes

Huh7.5 and HuS-E7/DN24 cells were separately infected with serums derived from 3 different HCV-patients or by JFH-1 concentrated medium (HCV-2a). Two serums were infected by HCV-1b, while the third by HCV-2b. Inoculated virus titer was adjusted to be the same in all cases. Except for JFH-1, which efficiently

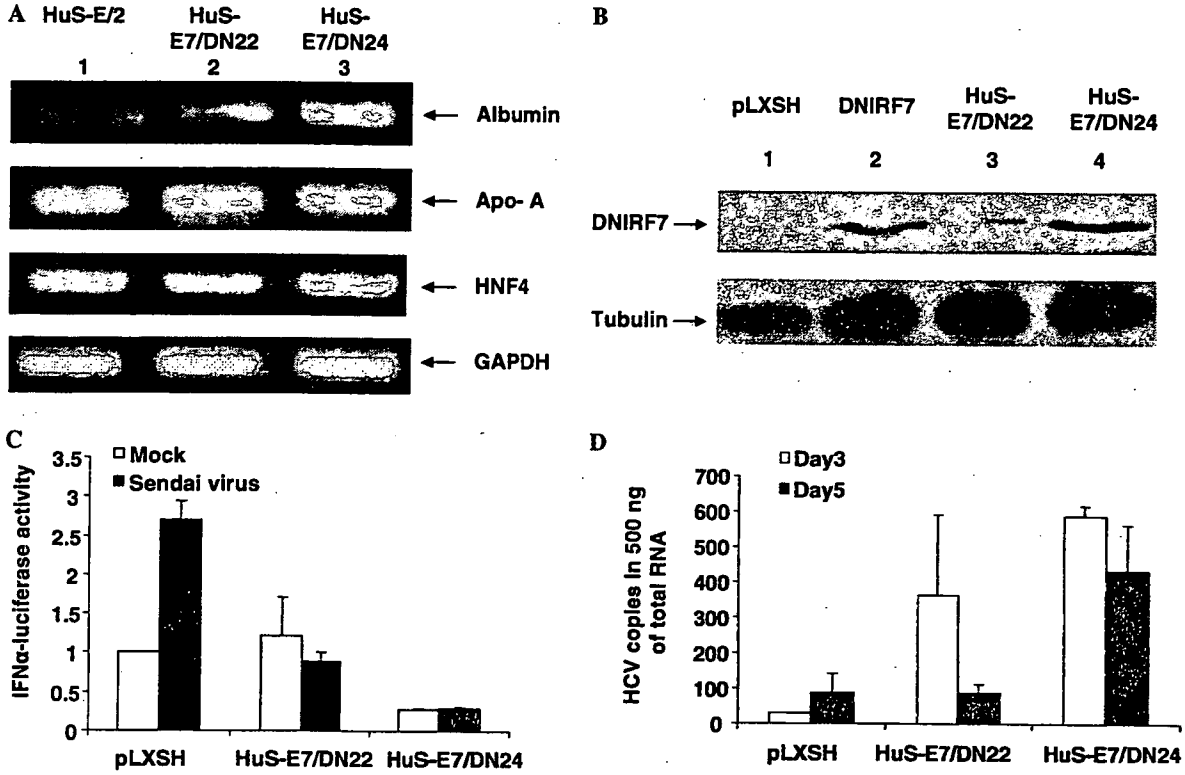

Fig. 6. (A) The pLXSH-HA-DNIRF-7 plasmid was transfected into HuS-E/2 cells, followed by selection in 100 μg/ml Hygromycin B. Two clones, HuS-E7/DN22 (lane 2) and HuS-E7/DN24 (lane 3), were obtained. We investigated the expression of albumin, apo-A, HNF4, and GAPDH as an internal control in parental HuS-E/2, HuS-E7/DN22, and HuS-E7/DN24 hepatocytes cultured for two weeks by RT-PCR. (B) Expression of HA-tagged DNIRF-7 (upper panel) and tubulin (control, lower panel) was detected by immunoblotting analysis. HuS-E/2 cells transiently transfected with either empty pLXSH vector (lane 1) or pLXSH-HA-DNIRF-7 (lane 2) were used as negative and positive controls, respectively, after 48 h. (C) HuS-E/2, HuS-E7/DN24, and HuS-E7/DN22 cells were transfected with IFNα-luc. HuS-E/2 cells were also cotransfected with pLXSH. All of these cells were then infected (black bar) or with Sendai virus or mock-infected, then analyzed for luciferase activity after 12 h. (D) HuS-E7/DN24 cells exhibited high infectivity to HCV samples derived from patient serum. HuS-E/2 cells were transiently transfected with empty pLXSH. Twenty-four hours later, serum from a recurrently transplanted HCV patient was used to infect transfected cells and HuS-E7/DN22 and HuS-E7/DN24 cells for 24 h. After washing three times, cells were cultured in fresh medium. Cells were then harvested and lysed at the indicated time points.

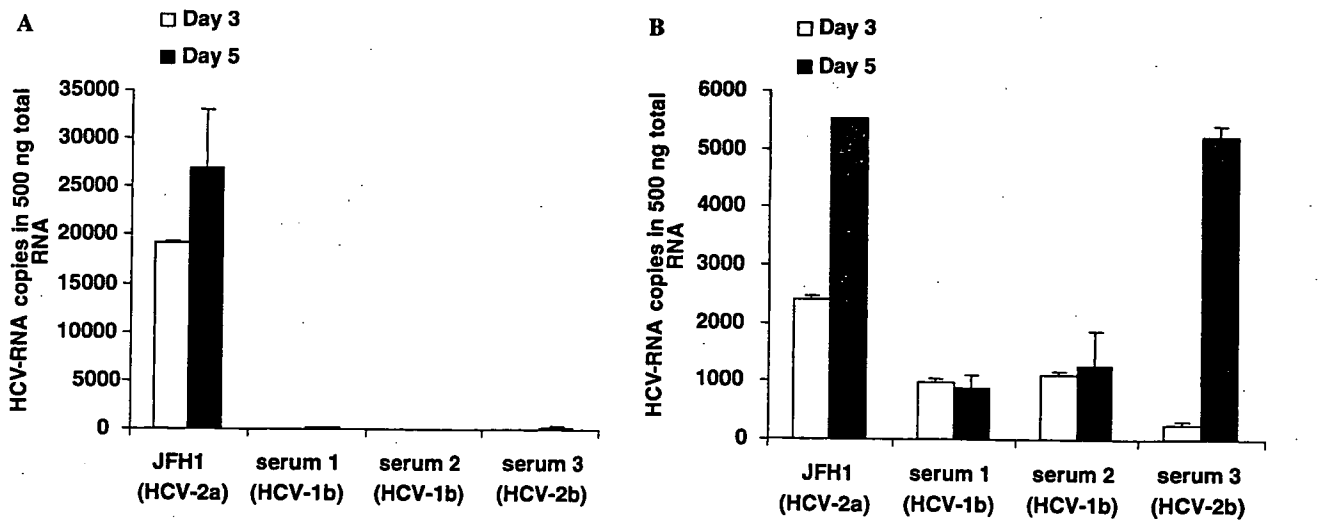

Fig. 7. The infectability of Huh-7.5 and HuS-E7/DN24 cells to different HCV genotypes. Huh-7.5 (A) and HuS-E7/DN24 (B) cells were infected with same titer of JFH1 (HCV-2a), two different HCV-1b serums and one HCV-2b serum. After removing the infected medium, the cells were washed in PBS and recultured in fresh medium. Cells were harvested and lysed at the indicated time points. The quantity of HCV genome RNA per 500 ng RNA was detected by real-time RT-PCR analysis.

replicated in Huh7.5 cells (Fig. 7A), HuS-E7/DN24 cells showed a higher and reproducible infectability for the different HCV strains than Huh7.5 cells (Fig. 7B). Similar higher infectability of HuS-E7/DN24 cells was observed with HCV-4a genotype (unpublished data). These results suggest that the high infectability of Huh-7.5 with JFH-1 is specific among the combinations of HCV strains and cell lines; while HuS-E7/DN24 cells were generally permissive to HCV-infected serum independent of HCV strains.

4. Discussion

This study demonstrates that ectopic expression of the HPV18/E6E7 genes in combination with hTERT could efficiently immortalize mature human hepatocytes, generating a cell line with stable expression of hepatocyte markers and functions for more than 30 weeks in culture. HuS-E/2 cells continuously exhibited higher expression of both HGF and HGFR than HuS-T/2 cells. This result suggests that HPV18/E6E7-immortalized hepatocytes maintain responsiveness to paracrine signals capable of inducing cell differentiation to a greater extent than SV40 T-immortalized hepatocytes. This conclusion is further supported by the increased expression of HNF4 in HuS-E/2 cells in comparison to HuS-T/2 cells. HNF4 is a major hepatocyte transcription factor, required for hepatocyte differentiation and liver-specific gene expression [26]. HNF4 drives hepatocytes differentiation by acting upstream in a transcription factor cascade that included HNF1α [27]. HuS-E/2 cells continued to express HNF1α throughout prolonged culture, while HuS-T/2 cells lost expression completely. Maintenance of hepatocellular functions was demonstrated by continuous and high expression of albumin, apolipoprotein-A, human transferrin, and E-cadherin by HuS-E/2 in comparison to HuS-T/2 cells. These differences became more pronounced in the late passages. In a similar manner, HuS-E/2 cells continued to express all of the examined CYP genes, with the exception of CYP 3A4, while HuS-T/2 cells lost expression of CYP 3A4, 1B, and 2E1 completely and displayed markedly lower expression of CYP 1B1 than HuS-E/2 cells. Thus, human hepatocytes immortalized by HPV E6/E7 transfection are phenotypically similar to primary hepatocytes, even during extended cultures.

Recently, it was reported that the JFH-1 strain and derived chimeras could only infect and propagate efficiently in Huh7.5.1 and Huh7.5 cells, both of which are subclones of Huh7 cells [7–9]. This limitation, however, may be specific to the JFH-1 strain, which may not accurately reflect the course of other HCV strains' infection. Thus, usage of HCV particles isolated from patient serum could be more useful to study authentic HCV infection. Using sera from HCV patients as a source of infective virus, HPV18/E6E7-immortalized cell lines exhibited higher reproducible susceptibility to HCV infection than HuS-T, PH5CH8, and Huh-7.5 cell lines.

IRF3 and IRF7 play an important role in the activation of interferon signaling [28]. We suppressed the functions of IRF-3 or IRF-7 to assess their role in HCV infectivity. In fact, we observed significant increase of HCV replication in HuS-E/2 cells bearing dominant-negative IRF7 that impaired IFN signaling. The suppression of IRF-3, however, did not have any significant effect on HCV infectivity or replication in this cell line. This may result from the blockade of IRF-3 activation by an HCV NS3/4A serine protease [29] through at least two independent pathways that inhibit the TLR3-dependent and RIG-I-dependent signaling pathways [29–33]. Although HCV was shown to inhibit basal expression levels of IRF-7 at both mRNA and protein levels and it was shown that NS5A suppresses IRF-7-induced IFNα promoter activation [34]. Stimulation of TLR7 was shown to activate IRF-7 and induce suppression of HCV replicon levels in Huh-7 cells [35]. This suggests that the inhibition of IRF7 by HCV is not complete. Using IRF-7-deficient (IRF-7−/−) mice, Honda [36] demonstrated that the transcription factor IRF-7 is essential for the induction of IFNα/β genes. We established a clone stably expressing DNIRF-7 (HuS-7E/DN24), which demonstrated higher infectivity with different HCV strains than the parental HuS-E/2 clone.

In summary, we have established a human hepatocyte-derived cell line that maintains the characteristic features of primary hepatocytes by transduction with HPV18/E6E7. This cell line is highly infectable by HCV, which suggests that these cells may be useful to characterize the molecular mechanisms involved with HCV infection and to develop novel HCV treatment modalities.

Acknowledgements

We thank Dr. Akagi at Osaka Bioscience Institute for providing hTERT expressing vector, Dr. Sakai at the Institute for Virus Research, Kyoto University, for providing HPV18/E6E7 expressing plasmid, and Dr. Taniguchi of the University of Tokyo for providing IFNβ, and IFNα promoters' reporter plasmids. This work was supported by Grants-in-Aid for cancer research and for the second-term comprehensive 10-year strategies for cancer control from the Ministry of Health, Labor and Welfare, by Grants-in-Aid for scientific research from the Ministry of Education, Culture, Sports, Science and Technology, by Grants-in-Aid for the research for the future program from the Japanese society for the Promotion of Science. Dr. Hussein H. Aly is a receiver of the Japanese *Gakushu Shoreihi* scholarship and was partly supported by Prof. *Yassin A. El Ghaffar memorial scholarship* for the Improvement of Liver research in Egypt.

References

[1] Wasley A, Alter MJ. Epidemiology of hepatitis C: geographic differences and temporal trends. Semin Liver Dis 2000;20:1–16.

[2] Manns MP, McHutchison JG, Gordon SC, Rustgi VK, Shiffman M, Reindollar R, et al. Peginterferon alfa-2b plus ribavirin compared with interferon alfa-2b plus ribavirin for initial treatment of chronic hepatitis C: a randomised trial. Lancet 2001;358:958–965.

[3] Fried MW, Shiffman ML, Reddy KR, Smith C, Marinos G, Goncales Jr FL, et al. Peginterferon alfa-2a plus ribavirin for chronic hepatitis C virus infection. N Engl J Med 2002;347: 975–982.

[4] Hadziyannis SJ, Sette Jr H, Morgan TR, Balan V, Diago M, Marcellin P, et al. Peginterferon-alpha2a and ribavirin combination therapy in chronic hepatitis C: a randomized study of treatment duration and ribavirin dose. Ann Intern Med 2004;140:346–355.

[5] Muir AJ, Bornstein JD, Killenberg PG. Peginterferon alfa-2b and ribavirin for the treatment of chronic hepatitis C in blacks and non-Hispanic whites. N Engl J Med 2004;350:2265–2271.

[6] Falck-Ytter Y, Kale H, Mullen KD, Sarbah SA, Sorescu L, McCullough AJ. Surprisingly small effect of antiviral treatment in patients with hepatitis C. Ann Intern Med 2002;136:288–292.

[7] Wakita T, Pietschmann T, Kato T, Date T, Miyamoto M, Zhao Z, et al. Production of infectious hepatitis C virus in tissue culture from a cloned viral genome. Nat Med 2005;11:791–796.

[8] Zhong J, Gastaminza P, Cheng G, Kapadia S, Kato T, Burton DR, et al. Robust hepatitis C virus infection in vitro. Proc Natl Acad Sci USA 2005;102:9294–9299.

[9] Lindenbach BD, Evans MJ, Syder AJ, Wolk B, Tellinghuisen TL, Liu CC, et al. Complete replication of hepatitis C virus in cell culture. Science 2005;309:623–626.

[10] Dellgado JP, Parouchev A, Allain JE, Pennarun G, Gauthier LR, Dutrillaux AM, et al. Long-term controlled immortalization of a primate hepatic progenitor cell line after Simian virus 40 T-Antigen gene transfer. Oncogene 2005;24:541–551.

[11] Mizuguchi T, Mitaka T, Katsuramaki T, Hirata K. Hepatocyte transplantation for total liver repopulation. J Hepatobiliary Pancreat Surg 2005;12:378–385.

[12] Isom HC, Tevethia MJ, Kreider JW. Tumorigenicity of simian virus 40-transformed rat hepatocytes. Cancer Res 1981;41: 2126–2134.

[13] Ray FA, Waltman MJ, Lehman JM, Little JB, Nickoloff JA, Kraemer PM. Identification of SV40 T-antigen mutants that alter T-antigen-induced chromosome damage in human fibroblasts. Cytometry 1998;31:242–250.

[14] Chen WH, Lai WF, Deng WP, Yang WK, Lo WC, Wu CC, et al. Tissue engineered cartilage using human articular chondrocytes immortalized by HPV-16 E6 and E7 genes. J Biomed Mater Res A 2006;76:512–520.

[15] Dimri G, Band H, Band V. Mammary epithelial cell transformation: insights from cell culture and mouse models. Breast Cancer Res 2005;7:171–179.

[16] Harms W, Rothamel T, Miller K, Harste G, Grassmann M, Heim A. Characterization of human myocardial fibroblasts immortalized by HPV16 E6–E7 genes. Exp Cell Res 2001;268:252–261.

[17] Shiga T, Shirasawa H, Shimizu K, Dezawa M, Masuda Y, Simizu B. Normal human fibroblasts immortalized by introduction of human papillomavirus type 16 (HPV-16) E6-E7 genes. Microbiol Immunol 1997;41:313–319.

[18] Akimov SS, Ramezani A, Hawley TS, Hawley RG. Bypass of senescence, immortalization, and transformation of human hematopoietic progenitor cells. Stem Cells 2005;23:1423–1433.

[19] Hung SC, Yang DM, Chang CF, Lin RJ, Wang JS, Low-Tone Ho L, et al. Immortalization without neoplastic transformation of human mesenchymal stem cells by transduction with HPV16 E6E7 genes. Int J Cancer 2004;110:313–319.

[20] Wang G, Johnson GA, Spencer TE, Bazer FW. Isolation, immortalization, and initial characterization of uterine cell lines: an in vitro model system for the porcine uterus. In vitro Cell Dev Biol Anim 2000;36:650–656.

[21] Hino H, Tateno C, Sato H, Yamasaki C, Katayama S, Kohashi T, et al. A long-term culture of human hepatocytes which show a high growth potential and express their differentiated phenotypes. Biochem Biophys Res Commun 1999;256:184–191.

[22] Watashi K, Hijikata M, Hosaka M, Yamaji M, Shimotohno K. Cyclosporin A suppresses replication of hepatitis C virus genome in cultured hepatocytes. Hepatology 2003;38:1282–1288.

[23] Murata T, Ohshima T, Yamaji M, Hosaka M, Miyanari Y, Hijikata M, et al. Suppression of hepatitis C virus replicon by TGF-beta. Virology 2005;331:407–417.

[24] Dasgupta A, Hughey R, Lancin P, Larue L, Moghe PV. E-cadherin synergistically induces hepatospecific phenotype and maturation of embryonic stem cells in conjunction with hepatotrophic factors. Biotechnol Bioeng 2005;92:257–266.

[25] Civas A, Island ML, Genin P, Morin P, Navarro S. Regulation of virus-induced interferon-A genes. Biochimie 2002;84:643–654.

[26] Ishiyama T, Kano J, Minami Y, Iijima T, Morishita Y, Noguchi M. Expression of HNFs and C/EBP alpha is correlated with immunocytochemical differentiation of cell lines derived from human hepatocellular carcinomas, hepatoblastomas and immortalized hepatocytes. Cancer Sci 2003;94:757–763.

[27] Wege H, Le HT, Chui MS, Liu L, Wu J, Giri R, et al. Telomerase reconstitution immortalizes human fetal hepatocytes without disrupting their differentiation potential. Gastroenterology 2003;124: 432–444.

[28] Mamane Y, Heylbroeck C, Genin P, Algarte M, Servant MJ, LePage C, et al. Interferon regulatory factors: the next generation. Gene 1999;237:1–14.

[29] Foy E, Li K, Wang C, Sumpter Jr R, Ikeda M, Lemon SM, et al. Regulation of interferon regulatory factor-3 by the hepatitis C virus serine protease. Science 2003;300:1145–1148.

[30] Sumpter Jr R, Loo YM, Foy E, Li K, Yoneyama M, Fujita T, et al. Regulating intracellular antiviral defense and permissiveness to hepatitis C virus RNA replication through a cellular RNA helicase, RIG-I. J Virol 2005;79:2689–2699.

[31] Breiman A, Grandvaux N, Lin R, Ottone C, Akira S, Yoneyama M, et al. Inhibition of RIG-I-dependent signaling to the interferon pathway during hepatitis C virus expression and restoration of signaling by IKKepsilon. J Virol 2005;79:3969–3978.

[32] Li K, Foy E, Ferreon JC, Nakamura M, Ferreon AC, Ikeda M, et al. Immune evasion by hepatitis C virus NS3/4A protease-mediated cleavage of the Toll-like receptor 3 adaptor protein TRIF. Proc Natl Acad Sci USA 2005;102:2992–2997.

[33] Foy E, Li K, Sumpter Jr R, Loo YM, Johnson CL, Wang C, et al. Control of antiviral defenses through hepatitis C virus disruption of retinoic acid-inducible gene-I signaling. Proc Natl Acad Sci USA 2005;102:2986–2991.

[34] Zhang T, Lin RT, Li Y, Douglas SD, Maxcey C, Ho C, et al. Hepatitis C virus inhibits intracellular interferon alpha expression in human hepatic cell lines. Hepatology 2005;42:819–827.

[35] Lee J, Wu CC, Lee KJ, Chuang TH, Katakura K, Liu YT, et al. Activation of anti-hepatitis C virus responses via Toll-like receptor 7. Proc Natl Acad Sci USA 2006;103:1828–1833.

[36] Honda K, Yanai H, Negishi H, Asagiri M, Sato M, Mizutani T, et al. IRF-7 is the master regulator of type-I interferon-dependent immune responses. Nature 2005;434:772–777.

DNA and its cationic lipid complexes induce CpG motif-dependent activation of murine dendritic cells

Takaharu Yoshinaga, Kei Yasuda, Yoshiyuki Ogawa, Makiya Nishikawa and Yoshinobu Takakura

Department of Biopharmaceutics and Drug Metabolism, Graduate School of Pharmaceutical Sciences, Kyoto University, Kyoto, Japan

doi:10.1111/j.1365-2567.2006.02451.x
Received 13 March 2006; revised 5 July 2006; accepted 5 July 2006.
Correspondence: Dr Y. Takakura, Department of Biopharmaceutics and Drug Metabolism, Graduate School of Pharmaceutical Sciences, Kyoto University, 46-29, Yoshidashimoadachi-cho, Sakyo-ku, Kyoto 606-8501, Japan.
Email: takakura@pharm.kyoto-u.ac.jp
Senior author: Yoshinobu Takakura

Summary

Unmethylated CpG motifs in bacterial DNA, but not in vertebrate DNA, are known to trigger an inflammatory response of antigen-presenting cells (APC). In this study, we investigated the cytokine release from murine dendritic cells (DC) by the addition of various types of DNA in the free or complexed form with cationic lipids. Naked plasmid DNA and *Escherichia coli* DNA with immunostimulatory unmethylated CpG motifs induced pro-inflammatory cytokine secretion from granulocyte–macrophage colony-stimulating factor (GM-CSF)-cultured bone marrow-derived DC and the DC cell-line, DC2.4 cells, though vertebrate calf thymus DNA (CT DNA) with less CpG motifs did not. These characteristics differed from mouse peritoneal resident macrophages that do not respond to any naked DNA. The amount of cytokines released from the DC was significantly increased by complex formation with cationic lipids when CpG-motif positive DNAs were used. Unlike murine macrophages or Flt-3 L cultured DC, GM-CSF DC did not release inflammatory cytokines in response to the addition of CT DNA/cationic lipid complex, suggesting that the activation is completely dependent on CpG motifs. Taken together, the results of the present study demonstrate that murine DC produce pro-inflammatory cytokines upon stimulation with CpG-containing DNAs and the responses are enhanced by cationic lipids. These results also suggest that DC are the major cells that respond to naked CpG DNA *in vivo*, although both DC and macrophages will release inflammatory cytokines after the administration of a DNA/cationic lipid complex.

Keywords: CpG motifs; dendritic cells; TLR9; DNA and DNA uptake

Introduction

It is well known that unmethylated CpG sequences (CpG motifs) in bacterial DNA, but not in vertebrate DNA, are recognized by the immune system as a danger signal.[1] Cytokines such as tumour necrosis factor-α (TNF-α), interleukin-6 (IL-6), IL-12 and interferon-α (IFN-α) are secreted from antigen presenting cells, especially macrophages or dendritic cells (DC), upon stimulation with CpG DNA and synthetic oligodeoxynucleotides (ODN) containing CpG motifs. These cytokines significantly modify the therapeutic effects of DNA-based therapies in different ways.[2] For example, in gene therapy, cytokine production generally seems inappropriate because these inflammatory cytokines significantly reduce transgene expression in target cells through their direct

Abbreviations: APC, antigen-presenting cells; DC, dendritic cells; BMDC, bone-marrow derived dendritic cell; CT DNA, calf thymus DNA; TNF-α, tumour necrosis factor-α; IL-6, interleukin-6; IL-12, interleukin-12; IFN-α, interferon-α; ELISA, enzyme-linked immunosorbent assay; FBS, fetal bovine serum; IRF, interferon regulatory factor; LPS, lipopolysaccharide; ODN, oligodeoxynucleotide; MHC, major histocompatibility complex; TLR, Toll-like receptor; JNK, c-Jun NH_2-terminal kinase; Flt-3 L DC, Flt-3ligand cultured bone-marrow dendritic cells; EC DNA, *Escherichia coli* DNA, pDNA, plasmid DNA; FL-pDNA, fluorescein labelled plasmid DNA; GM-CSF, DC; granulocyte–macrophage, colony-stimulating factor cultured dendritic cells; DNase II, deoxyribonuclease II.

cytotoxicity and promoter attenuation.[3–5] On the other hand, it is essential for DNA vaccination because these cytokines can enhance the immune responses and profoundly affect the balance of these cytokines and the nature of the immune responses.[6–9]

DC are one of the most important cell populations as far as both innate and acquired immunity are concerned. They influence a variety of immunological responses associated with the therapeutic use of CpG DNA.[10,11] In addition to cytokine secretion, the expression of surface major histocompatibility complex (MHC) class I and II molecules as well as costimulatory molecules increases, and the maturation of DC is induced upon stimulation with CpG motifs.[12] The initial important step for all these processes associated with CpG DNA is cellular uptake because the receptor of CpG DNA, Toll-like receptor-9 (TLR9), is expressed within cells.[13,14] Our previous *in vitro* study using a DC cell line, DC2.4 cells, in mice demonstrated that DC take up pDNA via a mechanism specific to some defined polyanions[15] similar to cultured mouse peritoneal macrophages.[16,17]

There is a rapidly growing body of information about the mechanism of antigen-presenting cell (APC) activation by CpG DNA. This activation requires endosomal acidification and recognition by TLR9.[18–20] CpG DNA appears to use a TLR9 signaling pathway for NF-κB and c-Jun NH_2-terminal kinase (JNK) and IRF-7 through MyD88.[19,21] However, these proposed mechanisms are mainly based on studies using synthetic phosphorothioate CpG ODN, and there is little information about the activation induced by native DNA. Our previous study has demonstrated that, in contrast to macrophage cell lines, primary cultured mouse peritoneal macrophages secrete almost no inflammatory cytokines upon stimulation with pDNA, in spite of extensive uptake of the CpG DNA[22]. However, DNA/cationic lipid complex can activate the murine macrophages to induce inflammatory cytokines, whether they have replete CpG motifs or not.[23] Flt-3-ligand cultured bone-marrow DC (Flt-3 L DC) exhibit a different type of activation.[24,25] Upon stimulation with naked DNA, bacterial pDNA and CpG ODN stimulate Flt-3 L DC to induce cytokines IFN-α or IL-6 although vertebrate CT DNA does not. However, TLR9 in Flt-3 L DC can react when CT DNA is combined with cationic lipid N-[1-(2,3-dioleoyloxy)propyl]-N,N,N-trimethylammonium methylsulfate (DOTAP).[24] Methylated CpG motifs or non-canonical CpG motifs complexed with DOTAP induce the activation of TLR9 in Flt-3 L DC. Further experiments have proved that the other sequences also induce the activation of TLR9 when ODNs are translocated to endosomes by DOTAP.[25] While receptor-mediated endocytosis restricts the uptake of DNA, adsorptive endocytosis by cationic lipids does not. Thus, enhancement of DNA uptake seems to control the activation of TLR9 by vertebrate DNA. In the present study, we used a different type of DC and showed that the cells could respond to only DNA with CpG motifs even if the DNA was translocated to endosomes by cationic lipids.

Materials and methods

Chemicals

RPMI-1640 medium was obtained from Nissui Pharmaceutical (Tokyo, Japan). *Escherichia coli* DNA (EC DNA) and calf thymus DNA (CT DNA) were purchased from Sigma (St Louis, MO). Lipofectin reagent and Opti-MEM were purchased from Invitrogen (Rockville, MD). Mouse recombinant GM-CSF (rGM-CSF) and Triton-X-114 were purchased from Nacalai Tesque (Kyoto, Japan). [α-^{32}P]dCTP (3000 Ci/mmol) was obtained from Amersham (Amersham, UK). Fetal Bovine Serum (FBS) was purchased from Thermo Trace (Melbourne, Australia).

Cell culture

Male ICR mice (5 weeks) were purchased from Shizuoka Agricultural Cooperative Association for Laboratory Animals (Shizuoka, Japan). After bone marrow was flushed out of the bones of the hind legs of the mice, the cells were cultured in RPMI-1640 medium supplemented with 10% fetal bovine serum (FBS) and 1000 U/ml rGM-CSF. After a 4–5 day incubation at 37° in 5% CO_2-95% air, cells were collected and centrifuged at 200 *g* for 10 min. After removal of the supernatant, the cells were resuspended in 400 μl phosphate-buffered saline (PBS) containing 0·5% bovine serum albumin (BSA) per 10^8 total cells. The cell suspension was mixed thoroughly with 100 μl magnetic-activated cell sorting (MACS) CD11c MicroBeads (Miltenyi Biotec, Germany), and incubated for 15 min at 4°. After incubation, the cells were washed, centrifuged at 200 *g* for 10 min, and resuspended in 500 μl PBS containing 0·5% BSA. Then, magnetic separation with MACS was carried out to isolate the DC by selecting CD11c-positive cells from the cultured cells. These isolated cells were washed and then plated on 24-well culture plates (Falcon, Becton Dickinson, Lincoln Park, NJ) at a density of 5×10^5 cells/well and cultured for 24 hr. The murine DC2.4 cells were a gift from Dr Kenneth Rock (Department of Pathology, University of Massachusetts Medical School, MA). DC2.4 cells display dendritic morphology, express dendritic cell-specific markers, MHC molecules, and costimulatory molecules, and exhibit phagocytic activity and an antigen-presenting capacity.[26] DC2.4 cells were cultured with RPMI-1640 medium supplemented with 10% FBS, 2 mM L-glutamine, 100 μM non-essential amino acids, 50 μM 2-mercaptoethanol, and antibiotics. They were then plated on a 24-well culture plate at a density of 5×10^5 cells/well and cultured for 24 hr.

DNA

pCMV-Luc encoding firefly luciferase gene was constructed, as described previously.[27] pDNA was purified using an Endo-free plasmid Giga kit (Qiagen, Valencia, CA). For the cellular association experiments, pDNA was radiolabelled with [α-^{32}P]dCTP by nick translation.[28] For the activation experiments, all DNA samples were extensively purified with Triton-X-114, a non-ionic detergent, to minimize the activation by contaminated lipopolysaccharide (LPS). Extraction of endotoxin from pDNA, EC DNA, and CT DNA samples was performed according to reviously published methods[29,30] with slight modifications. DNA samples were purified by extraction with phenol : chloroform : isoamyl alcohol (25 : 24 : 1) and ethanol precipitation. Then, 10 mg DNA was diluted with 20 ml pyrogen-free water, followed by the addition of 200 μl Triton-X-114 and mixing. The solution was placed on ice for 15 min and incubated for 15 min at 55°. Subsequently, the solution was centrifuged for 20 min at 25°, 600 *g*. The upper phase was transferred to a new tube, 200 μl Triton-X-114 was added, and the previous steps were repeated at least three times. The activity of LPS was measured by *Limulus* amoebocyte lysate (LAL) assay using the Limulus F Single Test kit (Wako, Tokyo, Japan). After purification using the Endo-free plasmid Giga kit, 1 μg/ml pDNA contained 0·01–0·05 EU/ml endotoxin. After Triton-X-114 extraction, the endotoxin levels of the DNA samples could no longer be determined by LAL assay, i.e. 1 μg/ml DNA contained less than 0·001 EU/ml. Without extraction of endotoxin by Triton-X-114, 100 μg/ml naked pDNA, which contains 1–5 EU/ml endotoxin, could release 521 ± 73 pg/ml TNF-α at 24 hr from peritoneal macrophages.

Cationic liposome formation

Lipofectin complexes were prepared according to the manufacturer's instructions. In brief, DNA was diluted in 100 μl Opti-MEM per 1 μg DNA (solution A) and 5 μl Lipofectin reagent was diluted in another 100 μl Opti-MEM (solution B). Then solutions A and B were combined and mixed gently. After a 15 min incubation at room temperature, complex was added to the cells.

Cellular association experiments

DC2.4 cells cultured in 24-well plates were washed three times with 0·5 ml Hanks' balanced salt solution (HBSS) without phenol red and 0·5 ml HBSS containing 0·1 μg/ml naked [^{32}P]pDNA or 0·1 μg/ml [^{32}P]pDNA/Lipofectin complex was added. After incubation at 37 or 4° for a specified time, the HBSS was removed and the cells were washed five times with ice-cold HBSS and then solubilized with 1·0 ml 0·3 N NaOH with 0·1% Triton-X-100. Aliquots of the cell lysate were taken for the determination of ^{32}P radioactivity using an LSA-500 scintillation counter (Beckman, Tokyo, Japan) and the protein content was measured using the modified Lowry method with BSA as a standard.

Confocal microscopy

DC2.4 cells were washed three times with 1·0 ml HBSS and incubated with HBSS containing fluorescein-labelled pDNA (FL-pDNA) or FL-pDNA/Lipofectin complex. After a 3 hr incubation, the cells were washed five times and fixed with 4% paraformaldehyde for 10 min.

Cytokine secretion

BMDC or DC2.4 cells cultured in 24-well plates were washed three times with 0·5 ml RPMI-1640 before use. Naked DNA was diluted in 0·5 ml Opti-MEM. The cells were incubated with the naked DNA solution continuously for 8 hr. In the case of DNA/Lipofectin complexes, cells were incubated for 2 hr with 0·5 ml of the solutions containing the complexes. Then, the cells were washed with RPMI-1640 and incubated with RPMI-1640 with 10% FBS. After a 6 hr incubation, the supernatant was collected for ELISA and kept at −80°. The levels of TNF-α, IL-6, and IL-12p70 in the supernatants were determined by the OptEIA Set (BD Biosciences, San Diego, CA).

Results

Uptake of DNA with cationic lipid complexes is not saturated, although normal uptake is saturated in GM-CSF DC

TLR9 exists in the endosomal-lysosomal compartment.[13,14] The amount of naked DNA in the compartment can be limited because naked DNA is supposed to be taken up by DC via receptor-mediated endocytosis.[15] However, DNA/cationic lipid complexes are supposed to be taken up by DC via a non-specific mechanism based on electrostatic interaction, so-called adsorptive endocytosis. Therefore, cationic lipid Lipofectin was used to deliver DNA efficiently to the compartment. To examine the binding and uptake of naked pDNA and pDNA/cationic lipid complexes in DC, we carried out cellular uptake experiments using naked [^{32}P]pDNA and [^{32}P]pDNA/Lipofectin complexes. As expected, the uptake of naked [^{32}P]pDNA by DC2.4 cells at 37° was increased up to 2 hr (Fig. 1a). Following an incubation of 2–5 hr, the amount of DNA remained unchanged, probably due to continued uptake and degradation.[15] On the other hand, complexation with cationic lipids enhanced the DNA uptake. Cationic lipids enhanced [^{32}P]pDNA binding and

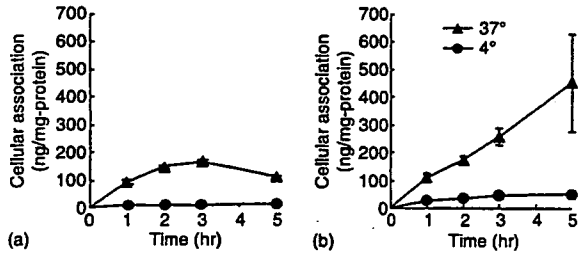

Figure 1. Cellular association time courses of naked [^{32}P]pDNA (a) or [^{32}P]pDNA/Lipofectin complex (b) in DC2.4 cells. Cells were incubated at 37° (closed triangle) or 4° (closed circle). Each point represents the mean ± SD (n = 3).

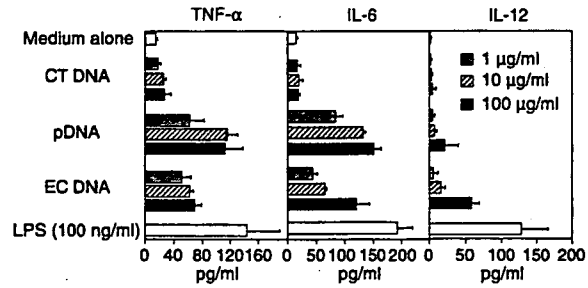

Figure 3. Cytokine secretion induced by naked DNA from GM-CSF DC. The cells were incubated with EC DNA, pDNA, or CT DNA for 8 hr. The supernatants were collected and the amount of TNF-α, IL-6, and IL-12 secreted from the cells was determined by ELISA. Each result represents the mean ± SD (n = 3).

uptake in DC2.4 cells and the amount of [^{32}P]pDNA increased in a time-dependent manner (Fig. 1b).

Next, we examined the localization of fluorescence-labelled DNA (FL-pDNA). In the confocal microscopy experiments, the fluorescence derived from naked FL-pDNA is bound to the cellular membrane at 4° (Fig. 2a). At 37°, FL-pDNA was observed inside the cells after 1 hr and it appeared to accumulate in the nucleus after a 3 hr incubation. On the other hand cationic lipids completely changed the localization of DNA. The fluorescence of the FL-pDNA/Lipofectin complex was observed in a punctuated pattern at 1 hr, then diffused into the cells after a 3 hr incubation (Fig. 2b).

The activation of GM-CSF DC by DNA

Next, cytokine production from DC by naked DNA was examined. Plasmid DNA and *E. coli* DNA were used as models of bacterial CpG DNA, and calf thymus DNA was used as a model of vertebrate DNA. As shown in Fig. 3, naked bacterial plasmid DNA and *E. coli* DNA with replete immunostimulatory CpG motifs induced TNF-α, IL-6 and IL-12 secretions from bone marrow-derived DC. The results are consistent with previous studies demonstrating that plasmid DNA stimulates GM-CSF DC to induce TNF-α and IL-12.[18] Vertebrate calf thymus DNA (CT DNA) containing less CpG motifs did not. LPS induced small amounts of cytokines, probably because of relatively short-term incubation (8 hr). Similar results were observed in the experiment using DC2.4 cells, although the cells released a higher amount of cytokines (Fig. 4). These results demonstrate that the cytokine secretion from the DC corresponds to the difference between endogenous DNA and exogenous DNA.

Next, cellular activation in DC by DNA/cationic lipid complexes was examined. The *E. coli* DNA/Lipofectin complexes stimulated GM-CSF cultured DC to produce cytokines, TNF-α, IL-6 and IL-12 in a dose-dependent manner (Fig. 5). Similar results were observed with pDNA/Lipofectin complex. The amounts of cytokines released from the DC were significantly increased by complex formation with cationic lipids compared with naked DNA (Fig. 3). The DC were unable to produce a significant amount of pro-inflammatory cytokines following

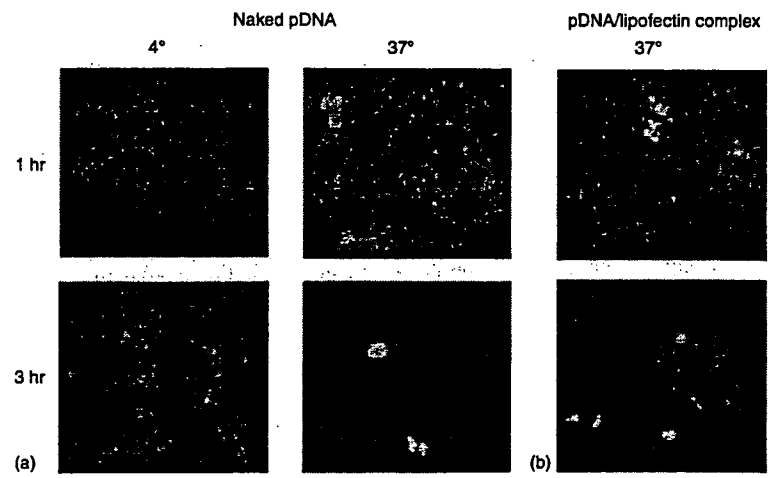

Figure 2. Uptake of naked FL-pDNA (a) or FL-pDNA/Lipofectin complex (b) by DC2.4 cells. The cells were incubated with 5·0 μg/ml naked FL-pDNA or 30 μg/ml FL-pDNA/Lipofectin complex.

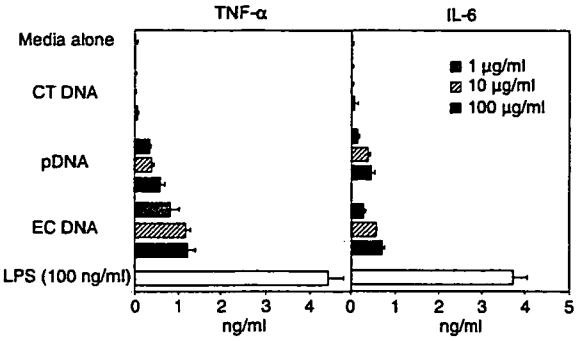

Figure 4. Cytokine secretion induced by naked DNA from DC2.4 cells. The cells were incubated with EC DNA, pDNA, or CT DNA for 8 hr. The supernatants were collected and the amount of TNF-α and IL-6 secreted from the cells was determined by ELISA. Each result represents the mean ± SD ($n = 3$).

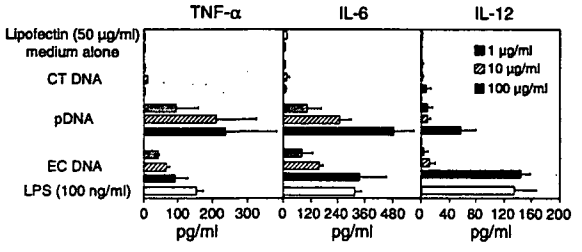

Figure 5. Cytokine secretion induced by DNA/Lipofectin complex from GM-CSF DC. The cells were incubated with EC DNA, pDNA, or CT DNA/Lipofectin complex (5 μl Lipofectin per 1 μg DNA). After a 2 hr incubation, liposomes were removed and fresh growth medium was added to the cells. The supernatants were collected 8 hr after the incubation with liposomes. The amount of TNF-α, IL-6, and IL-12 secreted from the cells was determined by ELISA. Each result represents the mean ± SD ($n = 3$).

stimulation with vertebrate calf thymus DNA (CT DNA) containing less CpG motifs when DNA is complexed to Lipofectin. Lipids alone were unable to stimulate the DC sufficiently to release pro-inflammatory cytokines. Similar results were obtained in DC2.4 cells (Fig. 6). These results demonstrate that GM-CSF DC discriminate between bacterial DNA and mammalian DNA.

Discussion

The most important role of immune system is to distinguish between 'self' and 'non-self'. Although the TLR9 subfamily (TLR7, 8 and 9) recognizes non-self nucleic acids[31] under special conditions, such as systemic lupus erythematosus, these TLRs are stimulated in response to self nucleic acids. For example chromatin–immunoglobulin complexes trigger DC activation in a TLR9-dependent and TLR9-independent manner.[32] Recently, Barton *et al.* have demonstrated that the fusion protein of

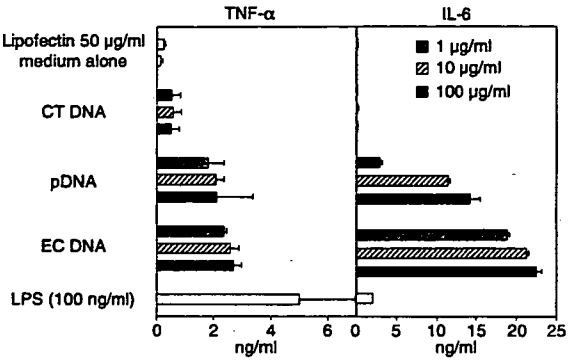

Figure 6. Cytokine secretion induced by DNA/Lipofectin complex from DC2.4 cells. The cells were incubated with EC DNA, pDNA, or CT DNA/Lipofectin complex (5 μl Lipofectin per 1 μg DNA). After a 2 hr incubation, liposomes were removed and fresh growth medium was added to the cells. The supernatants were collected 8 h after the incubation with liposomes. The amount of TNF-α and IL-6 secreted from the cells was determined by ELISA. Each result represents the mean ± SD ($n = 3$).

TLR4/9, which is delivered to cellular membranes, is activated by vertebrate DNA.[33] One proposed hypothesis is that compartmentalization of TLR9 prevents the response induced by endogenous DNA.

In the present study, we have demonstrated that GM-CSF-derived DC activation is triggered by exogenous naked DNA. Bacterial DNA induces cytokine secretion from DC, although vertebrate DNA does not. Flt-3 L cultured murine DC (Flt-3 L DC) also induce activation of TLR9 in response to naked bacterial DNA, but not naked vertebrate DNA.[24] Therefore, these studies imply that both GMCSF-DC and Flt-3 L DC can discriminate between bacterial non-self DNA and vertebrate self DNA.

On the other hand, these characteristics are different from murine macrophages.[22] Primary macrophages do not respond to naked DNA in spite of TLR9 expression, although the macrophage-like cell line RAW264.7 cells do. Both primary macrophages and DC take up DNA via a similar mechanism.[15–17] The mechanism of unresponsiveness of macrophages to DNA has not been elucidated, although TLR9 is present in the cells. Macrophages have deoxyribonuclease II (DNase II) in the lysosomal compartment, and they are responsible for apoptotic cell engulfment, DNA digestion and erythroid cell differentiation.[34] In erythropoiesis, macrophages take up nuclei and digest DNA. In DNase II-deficient mice, undigested DNA in macrophages causes IFN-β production via unknown receptors.[35] The cytokine production is mediated by the TLR9/MyD88 pathway and novel pathways that have been identified recently.[36,37] Therefore, the mechanism of the unresponsiveness of macrophages to naked DNA may involve the limited uptake and degradation by DNase II. However, further investigation is required.

The TLR4/9 fusion protein on the cell membrane is activated by vertebrate DNA.[33] This research indicates that compartmentalization into cells avoids TLR9 responses to endogenous DNA. Therefore, we forced DNA to internalize into cells using cationic lipids. In fact, vertebrate DNA/cationic lipid complexes can induce cytokine secretion from murine macrophages and Flt-3 L DC.[23,24] Following enhancement of DNA uptake by cationic lipids, these cells cannot distinguish between 'self' and 'non-self' DNA. In peritoneal macrophages, complexation of calf thymus DNA with cationic lipids elicited a similar level of inflammatory cytokine production to that obtained with bacterial *E. coli* DNA using cationic lipids.[23] In addition, calf thymus DNA with cationic lipid DOTAP causes a high degree of IFN-α release from murine Flt-3 L cultured DC or human peripheral blood mononuclear cells.[24] The amount of IFN-α induced by calf thymus DNA with DOTAP is similar to that induced by bacterial plasmid DNA. However, the result with GM-CSF DC is different from that in these cells. The cells only recognize bacterial DNA. Vertebrate DNA/cationic lipid complexes do not stimulate GM-CSF DC, although bacterial DNA does. There are two possibilities to explain these observations. One is the possibility that different types of cationic lipids lead to different forms of delivery of DNA, and result in different responses. For example, murine macrophages release inflammatory cytokines in response to the addition of vertebrate CT DNA/cationic lipid complexes.[23] Lipofectamine was used for this research. Synthetic double-stranded DNA containing no CpG motif can stimulate macrophage cell lines when DNA is complexed with the cationic lipid Fugene 6.[38] In addition, vertebrate CT DNA/cationic lipid Lipofectamine complexes induce macrophage activation via TLR9-dependent and -independent mechanisms.[39] Flt-3 L cultured DC (Flt-3 L DC) also responds to vertebrate DNA/cationic lipid DOTAP complexes via TLR9-dependent and -independent pathways.[24] TLR9-independent activation is also observed following transfection using Lipofectamine 2000.[37] Honda *et al.* showed that different cellular distributions of DNA result in different cytokine responses.[40] CpG-B ODN normally do not induce IFN-α release from plasmacytoid DC. However, following complexation with DOTAP, the same ODNs trigger IFN-α. Confocal microscopy reveals that DOTAP retains DNA in early endosomes, although ODNs without DOTAP are immediately transferred to lysosomal vesicles. Taken together, enhancement of the DNA uptake may not explain the response of TLR9 to vertebrate DNA and TLR9 may be present in specific compartments.

The other possibility is that GM-CSF DC, Flt-3 L DC and macrophages may contribute to the immune systems in different ways, by producing different types or degrees of induction. TLR9 is mainly expressed in B cells and plasmacytoid DC in humans.[31] On the other hand, mouse TLR9 is also present in myeloid DC and macrophages. Although further studies are required to clarify the contribution of DC or macrophages to immune responses *in vivo*, the present study suggests that DC are the main cells that respond to naked bacterial DNA, although both DC and macrophages will release inflammatory cytokines after the administration of bacterial DNA/cationic lipid complexes.

Very recently Martin *et al.* have shown that GM-CSF DC release type I IFN upon stimulation of mammalian DNA complexed with Fugene, another kind of lipid for transfection.[41] Interestingly, the cells do not produce TNF-α, IL-6 or IL-12. The activation is independent of TLR9 because GM-CSF DC from TLR9$^{-/-}$ deficient mice respond to mammalian DNA/Fugene complexes to secrete type I IFN. Another group has also demonstrated that non-CpG DNA/lipofectamine complexes stimulate GM-CSF DC to induce type I IFN.[42] The activation is not dependent on the MyD88 or TRIF pathways. Based on these observations, one can hypothesize that, distinct from Flt-3 L DC, GM-CSF DC respond to only bacterial or viral DNA via TLR9-dependent pathway, and release cytokines, such as TNF-α IL-6 and IL-12. However when mammalian DNAs are translocated into cells, GM-CSF DC may not induce these cytokines. Instead, the cells may release IFN-α through a TLR9-independent pathway. Further studies are required for these TLR9-dependent and -independent mechanisms.

In conclusion, the present study has demonstrated that murine GM-CSF DC or the DC cell line, DC2.4, produce pro-inflammatory cytokines following stimulation with CpG-containing DNAs and this production is increased when the DNAs are added to the cells in a complex form with cationic lipids. These findings form an important basis for future DNA-based therapies, including gene therapy and DNA vaccination.

Acknowledgements

This work was supported in part by 21st Century COE Program 'Knowledge Information Infrastructure for Genome Science', and also in part by a grant-in-aid for Scientific Research from the Ministry of Education, Culture, Sports, Science and Technology, Japan. We would like to thank Dr Kenneth Rock (Department of Pathology, University of Massachusetts Medical School, MA, USA) for providing DC2.4 cells.

References

1 Krieg AM. CpG motifs in bacterial DNA and their immune effects. *Annu Rev Immunol* 2002; 20:709–60.

2 Yasuda K, Wagner H, Takakura Y. Role of immunostimulatory DNA and TLR9 in gene therapy. *Crit Rev Ther Drug Carrier Syst* 2006; 23:89–110.

3 Haddad EB, Rousell J, Lindsay MA, Barnes PJ. Synergy between tumor necrosis factor alpha and interleukin 1beta in inducing transcriptional down-regulation of muscarinic M2 receptor gene expression. Involvement of protein kinase A and ceramide pathways. *J Biol Chem* 1996; 271:32586–92.

4 Qin L, Ding Y, Pahud DR, Chang E, Imperiale MJ, Bromberg JS. Promoter attenuation in gene therapy. interferon-gamma and tumor necrosis factor-alpha inhibit transgene expression. *Hum Gene Ther* 1997; 8:2019–29.

5 Sellins K, Fradkin L, Liggitt D, Dow S. Type I Interferons potently suppress gene expression following gene delivery using liposome (–) DNA complexes. *Mol Ther* 2005; 12:451–9.

6 Gurunathan S, Klinman DM, Seder RADNA vaccines: immunology, application, and optimization. *Annu Rev Immunol* 2000; 18:927–74.

7 Raz E, Tighe H, Sato Y *et al.* Preferential induction of a Th1 immune response and inhibition of specific IgE antibody formation by plasmid DNA immunization. *Proc Natl Acad Sci USA* 1996; 93:5141–5.

8 Roman M, Martin OE, Goodman JS *et al.* Immunostimulatory DNA sequences function as T helper-1-promoting adjuvants. *Nat Med* 1997; 3:849–54.

9 Seder RA, Hill AV. Vaccines against intracellular infections requiring cellular immunity. *Nature* 2000; 406:793–8.

10 Steinman RM, Dhodapkar M. Active immunization against cancer with dendritic cells: the near future. *Int J Cancer* 2001; 94:459–73.

11 Kadowaki N, Antonenko S, Liu YJ. Distinct CpG DNA and polyinosinic-polycytidylic acid double-stranded RNA, respectively, stimulate CD11c (–) type 2 dendritic cell precursors and CD11c (+) dendritic cells to produce type I IFN. *J Immunol* 2001; 166:2291–5.

12 Weiner GJ. The immunobiology and clinical potential of immunostimulatory CpG oligodeoxynucleotides. *J Leukoc Biol* 2000; 68:455–63.

13 Ahmad-Nejad P, Hacker H, Rutz M, Bauer S, Vabulas RM, Wagner H. Bacterial CpG-DNA and lipopolysaccharides activate Toll-like receptors at distinct cellular compartments. *Eur J Immunol* 2002; 32:1958–68.

14 Latz E, Schoenemeyer A, Visintin A *et al.* TLR9 signals after translocating from the ER to CpG DNA in the lysosome. *Nat Immunol* 2004; 5:190–8.

15 Yoshinaga T, Yasuda K, Ogawa Y, Takakura Y. Efficient uptake and rapid degradation of plasmid DNA by murine dendritic cells via a specific mechanism. *Biochem Biophys Res Commun* 2002; 299:389–94.

16 Takagi T, Hashiguchi M, Mahato RI, Tokuda H, Takakura Y, Hashida M. Involvement of specific mechanism in plasmid DNA uptake by mouse peritoneal macrophages. *Biochem Biophys Res Commun* 1998; 245:729–33.

17 Takakura Y, Takagi T, Hashiguchi M *et al.* Characterization of plasmid DNA binding and uptake by peritoneal macrophages from class A scavenger receptor knockout mice. *Pharm Res* 1999; 16:503–8.

18 Hacker H, Mischak M, Miethke T *et al.* CpG-DNA-specific activation of antigen-presenting cells requires stress kinase activity and is preceded by non-specific endocytosis and endosomal maturation. *EMBO J* 1998; 17:6230–40.

19 Yi AK, Tuetken R, Redford T, Waldschmidt M, Kirsch J, Krieg AM. CpG motifs in bacterial DNA activate leukocytes through the pH-dependent generation of reactive oxygen species. *J Immunol* 1998; 160:4755–61.

20 Hemmi H, Takeuchi O, Kawai T *et al.* A Toll-like receptor recognizes bacterial DNA. *Nature* 2000; 408:740–5.

21 Honda K, Yanai H, Mizutani T *et al.* Role of a transductional-transcriptional processor complex involving MyD88 and IRF-7 in Toll-like receptor signaling. *Proc Natl Acad Sci USA* 2004; 101:15416–21.

22 Yasuda K, Kawano H, Yamane I, Ogawa Y, Yoshinaga T, Nishikawa M, Takakura Y. Restricted cytokine production from mouse peritoneal macrophages in culture in spite of extensive uptake of plasmid DNA. *Immunology* 2004; 111:282–90.

23 Yasuda K, Ogawa Y, Kishimoto M, Takagi T, Hashida M, Takakura Y. Plasmid DNA activates murine macrophages to induce inflammatory cytokines in a CpG motif-independent manner by complex formation with cationic liposomes. *Biochem Biophys Res Commun* 2002; 293:344–8.

24 Yasuda KYuP, Kirschning CJ *et al.* Endosomal translocation of vertebrate DNA activates dendritic cells via TLR9-dependent and -independent pathways. *J Immunol* 2005; 174:6129–36.

25 Yasuda K, Rutz M, Schlatter B *et al.* CpG motif-independent activation of TLR9 upon endosomal translocation of 'natural' phosphodiester DNA. *Eur J Immunol* 2006; 36:431–6.

26 Shen Z, Reznikoff G, Dranoff G, Rock KL. Cloned dendritic cells can present exogenous antigens on both MHC class I and class II molecules. *J Immunol* 1997; 158:2723–30.

27 Nomura T, Yasuda K, Yamada T, Okamoto S, Mahato RI, Watanabe Y, Takakura Y, Hashida M. Gene expression and antitumor effects following direct interferon (IFN)-gamma gene transfer with naked plasmid DNA and DC-chol liposome complexes in mice. *Gene Ther* 1999; 6:121–9.

28 Sambrook J, Fritsch EF, Maniatis T *Molecular Cloning: a Laboratory Manual*, 2nd edn. Cold Spring Harbor, NY: Cold Spring. Harbor Laboratory Press, 1989.

29 Cotten M, Baker A, Saltik M, Wagner E, Buschle M. Lipopolysaccharide is a frequent contaminant of plasmid DNA preparations and can be toxic to primary human cells in the presence of adenovirus. *Gene Ther* 1994; 1:239–46.

30 Hartmann G, Krieg AM. CpG DNA and LPS induce distinct patterns of activation in human monocytes. *Gene Ther* 1999; 6:893–903.

31 Wagner H. The immunobiology of the TLR9 subfamily. *Trends Immunol* 2004; 25:381–6.

32 Boule MW, Broughton C, Mackay F, Akira S, Marshak-Rothstein A, Rifkin IR. Toll-like receptor 9-dependent and -independent dendritic cell activation by chromatin-immunoglobulin G complexes. *J Exp Med* 2004; 199:1631–40.

33 Barton GM, Kagan JC, Medzhitov R. Intracellular localization of Toll-like receptor 9 prevents recognition of self DNA but facilitates access to viral DNA. *Nat Immunol* 2006; 7:49–56.

34 Nagata S. DNA degradation in development and programmed cell death. *Annu Rev Immunol* 2005; 23:853–75.

35 Yoshida H, Okabe Y, Kawane K, Fukuyama H, Nagata S. Lethal anemia caused by interferon-beta produced in mouse embryos carrying undigested DNA. *Nat Immunol* 2005; 6:49–56.

36 Okabe Y, Kawane K, Akira S, Taniguchi T, Nagata S. Toll-like receptor-independent gene induction program activated by

mammalian DNA escaped from apoptotic DNA degradation. *J Exp Med* 2005; **202**:1333–9.

37 Ishii KJ, Coban C, Kato H *et al.* A Toll-like receptor-independent antiviral response induced by double-stranded B-form DNA. *Nat Immunol* 2006; **7**:40–8.

38 Zhu FG, Reich CF, Pisetsky DS. Effect of cytofectins on the immune response of murine macrophages to mammalian DNA. *Immunology* 2003; **109**:255–62.

39 Yasuda K, Ogawa Y, Yamane I, Nishikawa M, Takakura Y. Macrophage activation by a DNA/cationic liposome complex requires endosomal acidification and TLR9-dependent and -independent pathways. *J Leukoc Biol* 2005; **77**:71–9.

40 Honda K, Ohba Y, Yanai H, Negishi H, Mizutani T, Takaoka A, Taya C, Taniguchi T. Spatiotemporal regulation of MyD88-IRF-7 signaling for robust type-I interferon induction. *Nature* 2005; **434**:1035–40.

41 Martin DA, Elkon KB. Intracellular mammalian DNA stimulates myeloid dendritic cells to produce type I interferons predominantly through a toll-like receptor 9-independent pathway. *Arthritis Rheum* 2006; **54**:951–60.

42 Stetson DB, Medzhitov R. Recognition of cytosolic DNA activates an IRF3-dependent innate immune response. *Immunity* 2006; **24**:93–103.

J Gastroenterol 2006; 41:750–757
DOI 10.1007/s00535-006-1842-x

Journal of Gastroenterology

Negative regulation of intracellular hepatitis C virus replication by interferon regulatory factor 3

Tsuyoshi Yamashiro[1,3], Naoya Sakamoto[1], Masayuki Kurosaki[1], Nobuhiko Kanazawa[1], Yoko Tanabe[1], Mina Nakagawa[1], Cheng-Hsin Chen[1], Yasuhiro Itsui[1], Tomoyuki Koyama[1], Yoshie Takeda[1], Shinya Maekawa[1,2], Nobuyuki Enomoto[2], Hiroshi Sakugawa[3], and Mamoru Watanabe[1]

[1]Department of Gastroenterology and Hepatology, Tokyo Medical and Dental University, 1-5-45 Yushima, Bunkyo-ku, Tokyo 113-8519, Japan
[2]First Department of Internal Medicine, University of Yamanashi, Chuo, Japan
[3]First Department of Internal Medicine, School of Medicine, University of the Ryukyus, Okinawa, Japan

Editorial on page 814

Background. Interferon regulatory factor (IRF)-3 plays an important role in initiating cellular interferon-stimulated gene-mediated antiviral responses. In the present study, we evaluated the effects of IRF-3 expression and activation on intracellular hepatitis C virus (HCV) replication using an HCV replicon system. ***Methods.*** An HCV replicon was constructed that expressed a neomycin-selectable chimeric firefly luciferase reporter protein. A small interfering (si) RNA oligonucleotide directed against IRF-3 mRNA was designed and synthesized. A eukaryote expression plasmid vector was constructed that expressed IRF-3 mRNA under control of the cytomegalovirus early promoter/enhancer. To evaluate transcriptional activity of the interferon-stimulated genes, a reporter vector was used that expressed firefly luciferase under control of the interferon-stimulated response element (ISRE). ***Results.*** The baseline expression of IRF-3 did not significantly differ between cells with and without expression of the replicon. Transfection of an IRF-3 expression plasmid into the cells raised the ISRE-luciferase activities. The increase of ISRE activity was significantly more potent in the replicon-expressing cells than in cells without replicon expression. Concomitantly, the overexpression of IRF-3 suppressed HCV replication levels. In contrast, siRNA knockdown of IRF-3 suppressed ISRE activity by 38% ± 2%. Interestingly, the suppression of IRF-3 resulted in a significant increase of HCV replication, by up to twofold, depending on the IRF-3 suppression levels. ***Conclusions.*** IRF-3 negatively regulated intracellular HCV replication, and was partially activated in cells that expressed the HCV replicon. Thus, IRF-3 is a key molecule controlling HCV replication through modulation of host interferon gene responses.

Received: March 15, 2006 / Accepted: April 8, 2006
Reprint requests to: N. Sakamoto

Key words: hepatitis C virus, interferon regulatory factor 3

Introduction

Hepatitis C virus (HCV) is a worldwide health-care problem causing a spectrum of liver disease ranging from an asymptomatic carrier state to liver cirrhosis and hepatocellular carcinoma.[1] Currently available anti-HCV treatments are based on high-dose administration of a major antiviral cytokine, interferon (IFN)- . However, even with the most efficient regimen of pegylated interferon in combination with ribavirin, almost half of all cases are refractory to the treatment and fail to eradicate the virus.[2] Without the IFN therapy, HCV is associated with persistent infection and replication in the liver in spite of intact host immune systems; these features lead us to speculate that HCV escapes from or attenuates host antiviral responses.

Type I IFN plays a central role in eliminating viruses not only in therapeutic applications but also as a na-tural cellular antiviral defense mechanism.[3,4] IFNs mediate antiviral responses by inducing expression of interferon-stimulated genes (ISGs), including those encoding 2,5-oligoadenylate synthetase, double-stranded RNA-dependent protein kinase R, and MxA proteins, resulting in the degradation of cellular RNA, general repression of protein synthesis, and apoptotic cell death.[5] Also, a DNA microarray analysis of chimpanzee liver experimentally inoculated with HCV revealed that expression of ISGs, including those encoding cytokines and chemokines, was the principal reaction during the course of the viral infection and its clearance and that a considerable proportion of the genes were inducible by IFNs.[6]

The expressional control of ISGs is directed by receptor-mediated stimuli of type I IFNs.[7] Binding of

the IFNs onto their receptors activates receptor-associated janus kinases, which phosphorylate signal transducer and activator of transcription (STAT) 1 and STAT2. The phosphorylated STATs, 1 and 2, recruit IFN regulatory factor (IRF)-9 to form a complex with IFN-stimulated gene factor-3, which translocates to the nucleus, binds the IFN-stimulated response element (ISRE) located in the promoter/enhancer region of ISGs, and activates expression of ISGs.[3,4,8]

Other than by type I IFNs, expression of ISGs is controlled by binding ISRE with other molecules, including IRF-1, IRF-3, and IRF-7. Among them, IRF-3 is a transducer of virus-mediated signaling and plays a critical role in the induction of cellular antiviral responses.[8–11] IRF-3, which is ubiquitously expressed in the cytoplasm, is subjected to phosphorylation by virus infection, double-stranded RNA, and bacterial lipopolysaccharides. The phosphorylated IRF-3 forms a homodimer, translocates to the nucleus, and predominantly activates expression of the IFN- gene and certain ISGs.[4,12,13]

The IRF-3-mediated IFN pathway might be a target of viruses to counteract antiviral responses and to promote virus replication in the infected cells. Ebola virus, bovine diarrhea virus, and influenza A virus interfere with the activation of IRF-3 through interactions of their virus-encoded proteins.[14–16] In the case of HCV, some reports suggest interaction of virus proteins with the cellular IFN system. The viral NS5A protein has been reported to interfere with cellular IFN signaling.[17] It has recently been reported that HCV NS3/4A fusion protein blocks virus-induced activation of IRF-3.[18] Taken together, these findings indicate that IRF-3 is not only a key molecule of cellular innate immune responses but also might be a target of antiviral strategies. However, the mechanisms of IRF-3 activation by HCV infection in hepatocytes have not been explored yet, nor have the effects of the activated IRF-3 on HCV been satisfactorily studied.

An HCV subgenomic replicon is an in vitro model that simulates cellular autonomous replication of HCV genomic RNA. The development of the replicon system has partly overcome the problem of a lack of HCV replication models.[19] Replication of the HCV replicon can be abolished by treatment with small amounts of type I and type II IFNs,[20–22] suggesting intact IFN receptor-mediated cellular responses. However, in the absence of the exogenous interferon, persistent and high-level expression of the replicon has caused us to speculate that intracellular virus-induced antiviral responses become attenuated or malfunction as a result of the expression of viral proteins. We have previously reported that the baseline activity of ISG expression is substantially decreased in cells expressing replicon and that this decrease is partly attributable to the transcriptional suppression of IRF-1.[23] In the present study, we extended our observations by investigating the effects of IRF-3 expression and activation on HCV replication.

Materials and methods

Cell culture

A human hepatoma cell line, Huh7, was maintained in Dulbecco's modified minimal essential medium (Sigma, St. Louis, MO, USA) supplemented with 2mM L-glutamine and 10% fetal calf serum at 37°C under 5% CO_2. Huh7 cells expressing the HCV replicon were cultured in medium containing 300μg/ml G418 (Wako, Osaka, Japan).

HCV replicon constructs and transfected cell lines

An HCV subgenomic replicon plasmid, pHCVIbneodelS (designated pRep-N), was derived from an infectious HCV clone, HCV-N, genotype Ib.[22] The replicon pRep-N was reconstructed by replacing the neomycin phosphotransferase gene with a fusion gene comprising the firefly luciferase and neomycin phosphotransferase genes (pRep-Feo, Fig. 1).[24,25] RNA was synthesized from pRep-N and pRep-Feo using T7-polymerase (Promega, Madison, WI, USA) and transfected into Huh7 cells. After culture in the presence of G418, cell lines stably expressing the replicon were established (Huh7/Rep-N and Huh7/Rep-Feo, respectively). We have previously reported that firefly luciferase activities of Feo-replicon-expressing cells correlate well with HCV NS3, NS4A, and NS5A protein expression levels and with the replicon RNA expression levels.

Cured Huh7 cells

To establish cured Huh7 cells (cHuh7), from which replicon RNA was eliminated, Huh7/Rep-Feo was treated

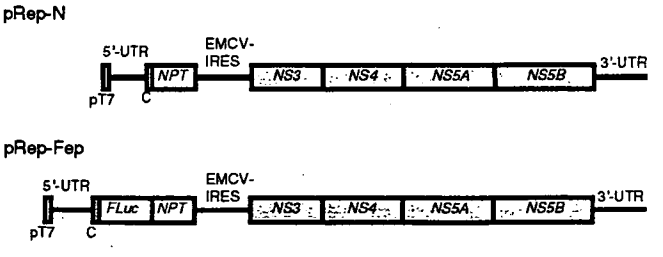

Fig. 1. Structures of the hepatitis C virus (HCV) replicon plasmids. *UTR*, untranslated region; *pT7*, T7 promoter; *C*, truncated HCV core region (nucleotides 342–377); *EMCV*, encephalomyocarditis virus; *Fluc*, firefly luciferase gene; *NPT*, neomycin phosphotransferase gene; *NS3*, *NS4*, *NS5A*, and *NS5B*, genes that encode HCV nonstructural proteins

with 100 U/ml of IFN- for 14 days. The absence of replicon RNA was confirmed by reverse transcriptase-polymerase chain reaction (RT-PCR) and by the loss of resistance to G418.[23]

Small interfering RNAs

Three small interfering RNAs (siRNAs) directed against IRF-3 were synthesized: siRNA1 (5 -gug gga gac agg acg cug cTT-3), siRNA2 (5 -gcc aga cac cuc ucc gga cTT-3), and siRNA3 (5 -ggu ugu gcc cac gug ccu cTT-3). A control siRNA was used as previously described (5 -ucg ggg cac ugc uag auc cTT-3).[24]

Plasmids

The expression plasmid vector pcDNA3.1-IRF-3 expresses the human IRF-3 open reading frame, which was cloned from human hepatocyte mRNA by RT-PCR using primers IRF-3/5 (5 -CAC CAT GGG AAC CCC AAA GCC ACG GAT CCT-3) and IRF-3/3 (5 -GCT CTC CCC AGG GCC CTG GAA ATC CAT G-3). The PCR product was inserted into the pcDNA3.1 TOPO vector (Invitrogen, Carlsbad, CA, USA) as instructed, and the nucleotide sequence was confirmed. The plasmid pcDNA3.1 (Invitrogen) was used as an empty vector for mock transfection. The plasmid pISRE-TA-Luc (Invitrogen) contained five copies of consensus ISRE motifs upstream of the firefly luciferase gene. pRL-CMV (Promega), which expressed *Renilla* luciferase protein, was used for correction of transfection efficiency.

Transient transfection

DNA and siRNA transfection was performed by using Lipofectamine 2000 (Invitrogen) according to the manufacturer's protocol. To perform reporter assays to determine the effect of IRF-3 on ISRE in the cells, a total of 5×10^4 Huh7, cHuh7, and Huh7/Rep-N cells were subcultured onto 24-well plates the day before transfection. A total of 100 ng of pISRE-TA-Luc and various amounts of pcDNA3.1-IRF-3 with empty vector and 0.1 ng of pRL-CMV, to a total mass of DNA of 400 ng, were transfected by using 2 µl of Lipofectamine 2000.

Western blotting

Cytoplasmic and nuclear fractions of cell lysates were prepared as described elsewhere.[26] The purity of the cytoplasmic and nuclear fractions was monitored by immunoblotting using an antibody directed against a nuclear protein, USF-2 (Santa Cruz Biotechnologies, Santa Cruz, CA, USA). Twenty micrograms of protein was separated using NuPAGE 4%–12% Bis-Tris gels (Invitrogen) and blotted onto an Immobilon polyvinylidene difluoride membrane (Roche). The membrane was immunoblotted with anti-IRF-3 (Santa Cruz) or anti-His antibodies (Invitrogen), and detected by chemiluminescence reaction (BM Chemiluminescence Blotting Substrate; Roche).

Immunocytochemical staining

Cells seeded onto tissue culture chamber slides were washed with phosphate-buffered saline (PBS) and fixed with 99% cold acetone for 10 min. After rinsing with PBS, cells were incubated with an anti-IRF-3 antibody at a dilution of 1/500 or an anti-His antibody at a dilution of 1/200 in PBS/3% goat serum. After 3 h, cells were washed three times with PBS, and incubated with fluorescein isothiocyanate (FITC)-labeled secondary antibodies. Cells were then washed and mounted with VectaShield mounting medium with 4 ,6-diamidino-2-phenylindole (DAPI; Vector Laboratories). Fluorescence microscopy was carried out with an Olympus BX50.

Luciferase reporter assays

Luciferase activity was measured by luminometer (Lumat LB9501; Promega) using a Bright-Glo Luciferase Assay System (Promega) or a Dual Luciferase Assay System (Promega). Assays were done in triplicate, and the results were expressed as means ± SD.

MTS assays

To evaluate cytotoxicity, MTS (dimethylthiazol carboxymethoxyphenyl sulfophenyl tetrazolium) assays were performed using a CellTiter 96 AQueous One Solution Cell Proliferation Assay (Promega) according to manufacturer's directions.

Statistical analyses

Statistical analyses were performed using an unpaired, two-tailed Student's *t* test; *P* values less than 0.05 were considered statistically significant.

Results

Expression level of IRF-3 in cells with and without HCV replication

First, we evaluated the expression levels of endogenous IRF-3 in Huh7 cells with or without expression of the HCV replicon. Western blotting analysis showed no sig-